University of Stavanger

Faculty of Science and Technology

MASTER'S THESIS

Study program/Specialization: **Petroleum Engineering/Drilling Technology**	Spring semester, 2016 **Open access** Open / Restricted access
Writer: **Igor Jovanov**	…… (Writer's signature)
Faculty supervisor: **Bernt Sigve Aadnoy** External supervisor(s):	
Thesis title: **Performance of autonomous inflow control systems**	
Credits (ECTS): **30**	
Key words: Inflow Control AICD ICD Principles Performance	Pages: 73 + enclosure: 9 (82 in total) Stavanger, 13. June, 2016 Date/year

Acknowledgements

I would like to thank supervisor Bernt Sigve Aadnøy, professor at the University of Stavanger, for providing me with his professional knowledge and expertise to complete this thesis work. I would also like to thank Terje Moen for providing the professional help and direct insight from the industry and Mesfin Belayneh Agonafir, professor at the University of Stavanger. They have been very helpful, by providing me with all the necessary knowledge and experience to finish this thesis. Last but not least, I would like to thank to my family and friends, here in Norway and back home in Serbia, who have given me an immense support, which helped to overcome this challenge.

Stavanger, 13. June, 2016

Igor Jovanov

Abstract

The first passive Inflow Control Devices (ICDs), were introduced in the early 1990's. Their task is to provide an additional choking effect in long reach horizontal wells and to eliminate heel-toe effect. There are several passive inflow control devices available today starting from the nozzle, helical/channel and tube type. Since none of them is able to provide additional choking effect, when the breakthrough occurs, the more advanced Autonomous Inflow Control Devices (AICDs) had to be developed. The primary function of any AICD is to be able to provide additional pressure drop when the breakthrough occurs, and unwanted fluids start flowing. There are some differences in the functionality and principles between available AICDs on todays market, and every device has its own range of abilities. Some of them are water and/or gas stopper valve, and some of them are flow controller valves. Water and gas stopper AICDs, are able to autonomously choke production of water and/or gas when it starts flowing, and allow oil producing zones to produce more easily, and most of them have the flow control ability in addition. On the other hand, flow controller AICDs are only regulating the flow rate, in order to keep it relatively constant or in predetermined limits. As a result, all of them have slightly different performance characteristics for different fluid types and flow properties.

This thesis covers the AICDs design, principles and performance characteristic of some of the available AICDs today. Principles on which their design is based on varies, some are implementing viscosity effects (Poiseuille's law), some density effect (Bernoulli's law), Bouyancy, Pressure sensitivity, etc. Based on that, they can be categorized as mainly viscosity dependent devices, pressure and flow rate sensitive devices, and buoyancy sensitive devices. It is shown how the performance characteristics vary between them, depending on the flowing fluid properties.

The results developed in this thesis, provide an insight in the available AICDs and their principles and performance. Therefore, it can be helpful in the process of making the decision on what is the best possible solution for inflow control system in the producing well.

Table of Contents

Acknowledgements i
Abstract ii
Table of Contents iii
List of Figures v
List of Tables vii
List of Abbreviations viii
1 Introduction 1
1.1 Development path from ICD to AICD 2
1.2 Scope of the Thesis 3
2 Autonomous Inflow Control Devices (AICDs) 4
2.1 Autonomous Flow Controller Device (AFD) 4
2.2 EquiFlow AICD 6
2.3 Equalizer Select AICD 9
2.4 Wormhole AICD 11
2.5 Counterweight Floating-Flapper Valve 13
2.6 Rate Controlled Production (RCP) Valve 15
2.7 Autonomous Inflow Control Valve (AICV) 19
3 Methodology 23
3.1 Performance Data Analysis (C, n) 24
4 Principles and Performances of AICDs 26
4.1 ICD nozzle Principle 26
4.1.1 ICD nozzle Performance 28
4.2 AFD Principles 29
4.2.1 AFD Performance 31
4.2.1.1 AFD valve vs. ICD Performance Comparison 32
4.3 EquiFlow AICD Principles 34
4.3.1 EquiFlow AICD Performance 35
4.3.1.1 EquiFlow vs. ICD Performance Comparison 37
4.4 Equalizer Select AICD Principles 39
4.4.1 Equalizer Select AICD Performance 40
4.4.1.1 Equalizer Select vs. ICD – nozzle Performance Comparison 43

4.5 Wormhole AICD Principles 45
4.5.1 Wormhole AICD Performance....46
4.6 Floating - Flapper Valve Principles....49
4.6.1 Floating – Flapper Valve Performance 51
4.7 RCP valve Principles....52
4.7.1 RCP valve Performance 53
4.7.1.1 RCP valve vs. ICD Performance Comparison....55
4.8 AICV Principles 57
4.8.1 AICV Performance....60
4.8.1.1 AICV vs. ICD – nozzle Performance Comparison....62
5 Discussion....64
5.1 AICD Comparison....64
5.2 Discussion of the Performance Data for AICDs 66
5.3 AICDs Sensitivity to the Different Reservoir Properties 68
5.4 Overview of Analyzed AICDs 69
6 Conclusion....70
7 References....71

List of Figures

Figure 1: Water breakthrough in the heel region of the well, (Bowen & Aadnoy, 2014) 1
Figure 2: Even drainage with the ICD completion, (Bowen & Aadnoy, 2014) 2
Figure 3: AFD, (Bowen & Aadnoy, 2014) 5
Figure 4: Performance curves for standard ICD (green) and for AFD (blue), (Bowen & Aadnoy, 2014) 6
Figure 5: AICD oil flow path (left) and water flow path (right), (Iqbal et al., 2015) 7
Figure 6: Measured flow through fluidic-diode type AICD, (Fripp et al., 2013) 8
Figure 7: Flow Path through Equalizer Select, (Akbari et al., 2014) 9
Figure 8: Autonomous Geometry of the Equalizer Select, (Akbari et al., 2014) 10
Figure 9: Relation between pressure drop coefficient and Reynolds number, (Banerjee et al., 2013) 11
Figure 10: Schematic of Adaptable Flow Control System Operation, (Delia et al., 2015) 12
Figure 11: Pressure Drop with Flowrate in the System, (Delia et al., 2015) 12
Figure 12: Floating flapper type valve, (Crow et al., 2006) 13
Figure 13: Counterweight Flapper Design, (Crow et al., 2006) 14
Figure 14: Statoil's RCP valve, profile picture, (Halvorsen et al., 2012) 15
Figure 15: Schematic picture of the RCP valve, (Halvorsen et al., 2012) 16
Figure 16: Sketch of the RCP valve with typical streamlines, (Halvorsen et al., 2012) 16
Figure 17: Cross section of valve and pressure profile at disc in closed position, (Halvorsen et al., 2012) 18
Figure 18: Volume flow of heavy oil, water and gas through RCP as a function of differential pressure, (Halvorsen et al., 2012) 19
Figure 19: Combination of laminar and turbulent flow restrictors in series, (Aakre et al., 2014) 20
Figure 20: AICV in open position, (Aakre et al., 2013) 21
Figure 21: AICV in close position, (Aakre et al., 2013) 21
Figure 22: Oil and gas flow through the ICD and AICV versus differential pressure, (Aakre et al., 2013) .. 22
Figure 23: Performance curves for ICD nozzle, pressure drop dependence on flow rate 28
Figure 24: AFD valve configuration, (Bowen & Aadnoy, 2014) 30
Figure 25: Performance curve for flow of oil (849 kg/m^3, 5 cP) through AFD valve, pressure drop dependence of fluid flow, (Bowen & Aadnoy, 2014) 31
Figure 26: Performance curve for flow of oil (890 kg/m^3, 121 cP) through AFD valve, pressure drop dependence of fluid flow, (Bowen & Aadnoy, 2014) 32
Figure 27: Comparison between flow of light oil through AFD and ICD – nozzle, (Bowen & Aadnoy, 2014) 33
Figure 28: Comparison between flow of heavy oil through AFD and ICD – nozzle, (Bowen & Aadnoy, 2014) 34
Figure 29: Tangential and radial pathways in EquiFlow, (Greci et al., 2014) 35
Figure 30: Performance curves for EquiFlow AICD, pressure drop dependence of fluid flow 36
Figure 31: Comparison between EquiFlow and ICD - nozzle performance characteristics 38
Figure 32: Flow paths through Equalizer Select AICD, (Abdelfattah et al., 2012) 39
Figure 33: Performance curves for Equalizer Select AICD, pressure drop dependence of flow rate, (Akbari, 2014) 41
Figure 34: Pressure loss coefficient (K) dependence on FRR setting of Equalizer Select AICD and Reynolds Number, (Akbari, 2014) 42
Figure 35: Comparison between Equalizer Select and ICD - nozzle performance characteristics 44
Figure 36: Wormhole AICD, with four labyrinth type pressure drop pathways, and four shut off valves, (Delia et al., 2015) 45
Figure 37: Shut off valve design, on the left three-dimensional model of the valve; on the right valve gate retaining component; (1 – valve saddle; 2 – valve cap; 3 – gate; 4 – magnets), (Volkov et al., 2014) 46
Figure 38: Performance curve for liquid (water) flow through Wormhole AICD, pressure drop dependence of flow rate, (Delia et al., 2015) 47
Figure 39: Performance curve for gas (air) flow through Wormhole AICD, pressure drop dependence of flow rate, (Delia et al., 2015) 48

Figure 40: Floating - Flapper valve working principle, force balance, (Crow et al., 2006) 49
Figure 41: Performance curves for Floating - Flapper Valve, pressure drop dependence of flow rate 51
Figure 42: Cross sectional schematic view of RCP valve, with pressure distribution through the device, (Isma Mohd, 2014) 52
Figure 43: Performance curves for RCP – valve, pressure drop dependence of flow rate 54
Figure 44: Comparison between RCP valve and ICD - nozzle performance characteristics 56
Figure 45: Pressure Drop vs. Velocity through the laminar flow restrictor, (Aakre et al., 2013) 58
Figure 46: Pressure Drop vs. Velocity through the turbulent restrictor, (Aakre et al., 2013) 58
Figure 47: AICV schematic view, showing main operational parts of the device, (Mathiesen et al., 2014) 60
Figure 48: Performance curves for AICV, pressure drop dependence of flow rate 61
Figure 49: Comparison between AICV and ICD - nozzle performance characteristics 63
Figure 50: Performance Comparison between AICV, RCP and EquiFlow 65

List of Tables

Table 1: Performance data (C, n), for ICD - nozzle 29
Table 2: Performance data (C, n), for EquiFlow AICD 37
Table 3: Available FRR settings, (Abdelfattah et al., 2012) 39
Table 4: Performance data (C, c), for Equalizer Select AICD 43
Table 5: Performance data (C, n), for RCP valve 55
Table 6: Performance data (C, n), for AICV 62
Table 7: Performance data (C, n), comparison for AICDs and ICD 66
Table 8: Final overview of the AICDs together with ICD 69

List of Abbreviations

ICD	Inflow Control Device
AICD	Autonomous Inflow Control Device
WC	Water Cut
GOR	Gas – Oil Ratio
AICV	Autonomous Inflow Control Valve
AFD	Autonomous Flow Controller Device
FRR	Flow Resistance Rating
RCP	Rate Controlled Production
AICV	Autonomous Inflow Control Valve
NCS	Norwegian Continental Shelf
PICD	Passive Inflow Control Device
BF	Buoyancy Factor

1 Introduction

The concept of Inflow Control Device (ICD) was developed firstly in the early 1990's. The necessity for ICD completion came from the uneven production from long horizontal wells. After investigations, it has been discovered that the long horizontal wells didn't necessarily produce much more compared to the horizontal wells with lower reach. The problem was that heel region of the well produced with higher flow rates compared to the toe region. The heel-toe effect (Ellis et al., 2009) for long horizontal wells is caused by the frictional well bore pressure drop, for fluid flowing from toe to heel region of the well. Therefore, decreasing the well bore pressure in the heel region of the wall, which leads to higher flow rate in the heel region. Caused by the increased flow rate, an early breakthrough was inevitable in the heel region of the well (Figure 1).

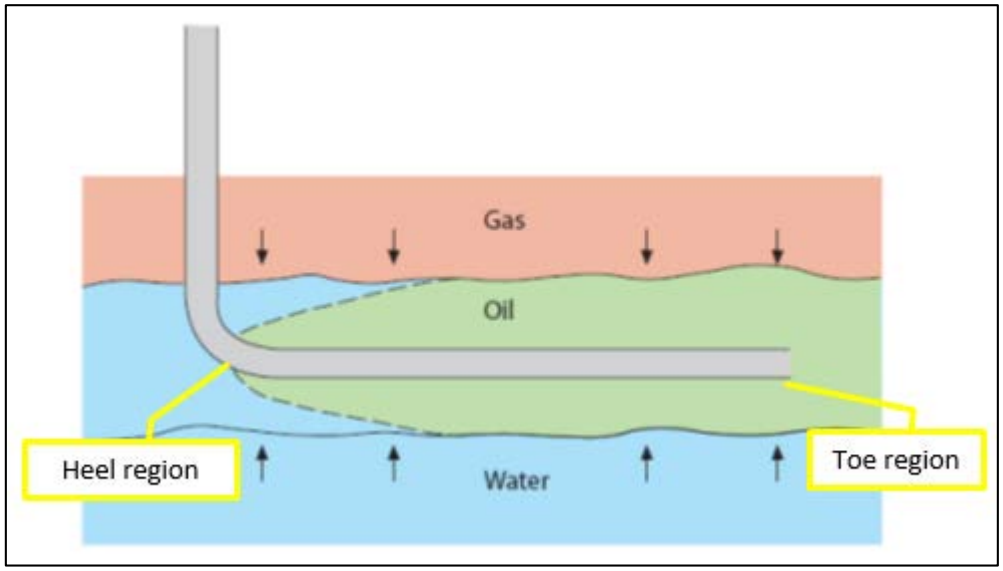

Figure 1: Water breakthrough in the heel region of the well, (Bowen & Aadnoy, 2014)

Firstly, the breakthrough problem was solved by installing the completion with the ICDs in place (Figure 2).

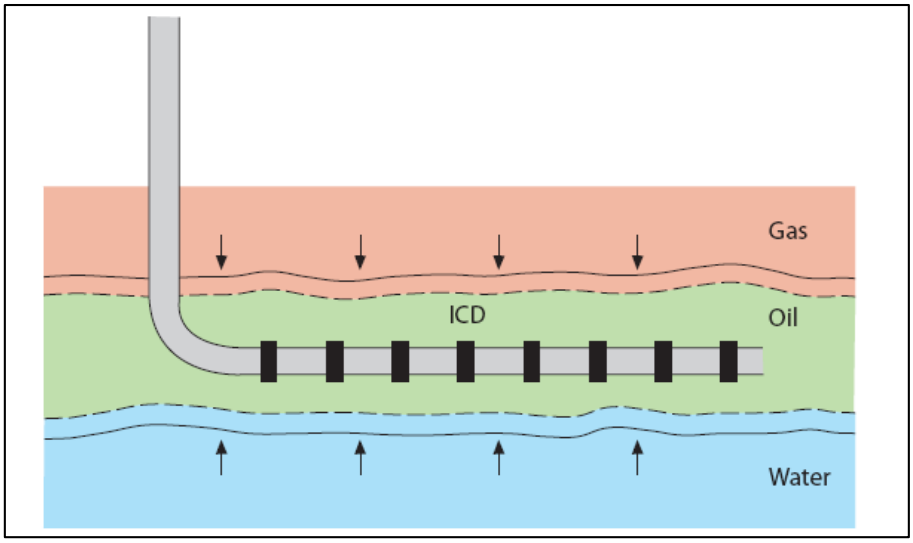

Figure 2: Even drainage with the ICD completion, (Bowen & Aadnoy, 2014)

With this kind of completion, with ICDs installed for inflow control, the breakthrough is slowed down, but when it happens, ICD is not efficient enough. In the event of a breakthrough, with the inflow of the unwanted fluids, ICD will provide only a limited amount of choking to the fluids with higher mobility. Water as a fluid with lower viscosity and gas as a fluid with lower density and viscosity, are more mobile compared to oil. Therefore, the ICD is not capable to provide higher choking effect for water and gas, and to stop or slow down the breakthrough. The biggest problem with an early breakthrough is in the thin oil reservoirs, where the contacts between different phases is close. Sweep efficiency of those reservoirs, will be decreased due to the breakthrough. This was the reason to pursue the development towards the autonomous inflow control devices (AICDs).

1.1 Development path from ICD to AICD

Firstly, the range of more advanced passive ICDs is developed. Going from regular ICD which design uses simple fluid dynamic principles for flow through a nozzle. Next ones included frictional pressure loss for flow through a pipe principle, together with pressure drop due to the flow through the nozzle. These traditional designs can be divided into several categories. Starting from nozzle ICDs (flow separation), channel/helix type of ICD (mainly frictional losses), and tube ICDs (combination of frictional losses) (Mayer et al., 2014). Once these devices are installed in the well completion, their properties can not be changed. Therefore, these device are categorized as “passive” inflow control devices (PICDs) by the industry.

Since the PICD were still not able to provide the necessary choking performance for different types of fluids, development led to the introducing of AICDs. Their design enables them to cope with the issue with undesirable fluid breakthrough (Aakre et al., 2013; L. Garcia et al., 2009; Least, Greci, Konopczynski, et al., 2013; Mathiesen et al., 2011). Because they are able to provide selective choking effect based on the flow of different fluids, they are called "autonomous" ICDs (AICDs) (Aakre et al., 2013; L. Garcia et al., 2009; Least, Greci, Konopczynski, et al., 2013). Based on the content of unwanted fluids, for example, high water cut (WC) or Gas-Oil ratio (GOR), additional choking is currently provided using two different approaches. First approach uses selective flow paths depending on the difference between inertial versus viscous drag forces (Fripp et al., 2013; Least, Greci, Konopczynski, et al., 2013). Second approach uses the principle of fluid flowing through a restriction (e.g. nozzle) and have an effect on a floating disc by generating a suction force on the disc, and pulling it towards the restriction due to the pressure difference between the top (suction side) and bottom surface of the disc (Aakre et al., 2013; Mathiesen et al., 2011). And one more approach for some of the available AICDs is based on the flowrate, and are acting as flow rate controller valves, therefore keeping the flow rate relatively constant (Bowen & Aadnoy, 2014; Delia et al., 2015).

1.2 Scope of the Thesis

In this Thesis, the idea behind it, is to evaluate the principles involved in the AICDs design and to evaluate their flow performance characteristics. In the chapters to follow, the process will involve firstly, introduction about the ACIDs, and afterwards a mathematical approach, in order to analyze the experimental data, behind the covered AICDs. By doing that, performance diagrams are going to be developed for each one of them, so their performance characteristics can be compared to regular ICD – nozzle, and in between.

Results should be able to show what are the main advantages and weaknesses of the AICDs covered in this thesis. By doing that, the devices are going to be categorized, based on their flow performance, under what reservoir fluid properties they can be used and what it is their optimal range of usage.

2 Autonomous Inflow Control Devices (AICDs)

AICDs were developed as a next step from passive inflow control devices (ICDs), combining passive inflow control element with an active inflow control element into one device. Passive element of the device ensures that the inflow is choked like with the regular ICD, by doing that it is slowing down the water or gas breakthrough occurrence (flow control). Active element ensures that the differential pressure across the AICD area is connected to fluid properties, composition and also with flow rate of the flowing fluid, when the water or gas breakthrough happens (Eltaher et al., 2014). By achieving these properties, AICD devices will choke more the zones where the breakthrough of gas or water has occurred, and will continue to produce from other zones normally.

As the properties of the fluid changes, the device reacts autonomously by changing the geometry of the fluid flow path or altering the flow path itself as a function of the controlling properties. AICDs don't require any connection from the surface in order to control the inflow, they are completely autonomous.

There are a few types of AICDs available today, depending on their functional properties they can be divided into two categories, depending if they can choke water and/or gas more than oil, and flow controller devices. Also, there are some newer inventions like the autonomous inflow control valves (AICV), which are designed to almost completely stop the inflow of gas when it occurs, by closing the valve autonomously. The next section will cover some of the available AICDs.

2.1 Autonomous Flow Controller Device (AFD)

The device is an autonomous, downhole flow regulator device constructed to control the inflow or outflow of fluids from the production or injection well as desired. The AFD valve is a "flow regulator" based on: hydraulic feedback principle with control provided by the Bernoulli Principle. This patented technology consists of a valve and valve body inserted into the completion equipment in the orientation required for production or injection mode (Bowen & Aadnoy, 2014).

Figure 3 shows a production well completed with sand control equipment, where the flow goes through a slot in the valve body housing allowing the bottom hole pressure (P1) to flow. When the production fluid has gone through the filter media (screen) it acts on top of the valve where the largest piston area will register this pressure (Bowen & Aadnoy,

2014). The same pressure, P1, in Figure 1 acts on the smaller area beneath the valve, where a spring is positioned. The difference between these two forces works against the spring force with a known constant, K, allowing the valve to move as needed, in order to maintain a constant flow rate during production or injection (Bowen & Aadnoy, 2014). All along the production interval of a well, the AFD will operate constantly, regarding flow performance, as well as when the reservoir pressure starts to drop. With an injection well, the valve is fixed at the predetermined injection rates and will stop any larger flow larger to go through every unit installed in a well.

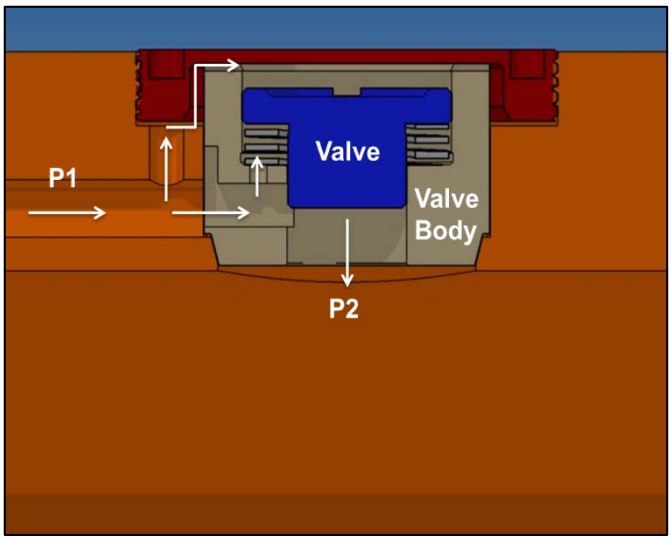

Figure 3: AFD, (Bowen & Aadnoy, 2014)

Figure 4 shows the performance curves of a standard ICD in comparison with the performance of the AFD. As observed, the ICD shows a decrease in flow rate with the decrease in pressure drop, whereas the AFD shows a fairly constant flow (Bowen & Aadnoy, 2014).

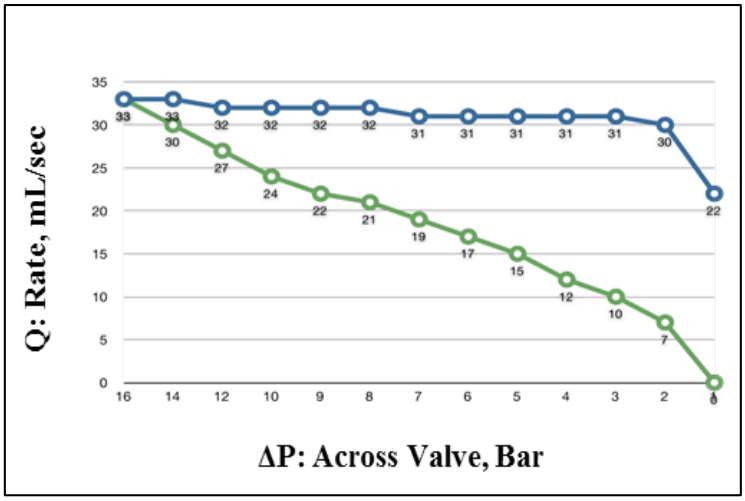

Figure 4: Performance curves for standard ICD (green) and for AFD (blue), (Bowen & Aadnoy, 2014)

2.2 EquiFlow AICD

Halliburton's EquiFlow AICD, is an inflow control device based on fluidic diode principle, without any moving parts, where the potential energy conversion of the flowing fluid is connected with the composition of the fluid and its properties like density, viscosity or flow rate. Controlling property of the device is achieved by modifying the flow path of the fluid or its geometry (Fripp et al., 2013).

An AICD must accomplish two principal tasks (Fripp et al., 2013):

1) It must determine whether the production fluid is mostly oil or whether it is mostly water and gas (Fripp et al., 2013);
2) It must restrict the production when the fluid is mostly water and gas (Fripp et al., 2013).

The controlling function of the EquiFlow AICD is achieved by conducting the different fluids through different pathways inside the device. The most important properties of the fluid, on which the design of this device is based on, are density, viscosity and flow rate. Density and flow rate of the fluid characterize the inertial forces, while viscosity and also flowrate of the fluid characterize the viscous forces. The AICD operates by using a balance between the inertial forces and the viscous forces in the fluid (Fripp et al., 2013).

When the inertial forces are predominant, the flow will favor to carry flowing through straight (tangential) pathway, and enter the vortex bowl with high angular momentum which will increase rotation and the pressure drop of the fluid flowing inside the AICD. On the other hand, with predominant viscous forces the flow will tend to split the flow

through all available pathways, divergent (radial) and straight (tangential). Thereby, the angular momentum between both pathways will be more or less balanced, which will minimize the rotation of the fluid in the AICD, and minimize the pressure drop and choking effect. Figure 5 shows that water and/or gas will carry through straight (tangential) pathway due to the higher inertial forces and lower viscosity, and will circumvent divergent (radial) pathway. And the oil, because it is more viscous fluid than water or gas, has predominant viscous forces and therefore will favor to go through both pathways (Fripp et al., 2013).

Figure 5: AICD oil flow path (left) and water flow path (right), (Iqbal et al., 2015)

In an actual produced reservoir fluid (oil and water), the effectiveness of the AICD is based on two factors (Iqbal et al., 2015):

1) Viscosity difference between two fluids (Iqbal et al., 2015);
2) Relative volumes of the two fluids (Iqbal et al., 2015).

The actual flow performance of the EquiFlow AICD can be compared to a valve which autonomously changes position to increase the choking effect when unwanted fluids start to flow. When the water starts flowing through the single AICD the water cut will not change, but the choking effect will, which will result with reduced flow from that zone and the balanced influx throughout the well. The result is maximized reservoir sweep and ultimate recovery.

Figure 6 shows one of the testing results done with the hot water and the 60 cP oil, which proves the pre stated principle, especially with heavy oils, that the pressure drop with oil flow is smaller, because oil does not rotate inside the vortex basin as much as water does. Water as a result of high angular velocity, creates also high velocity at the exit from AICD, which lead to a small period of back pressure and choking effect on water-producing zones.

This is not the case with oil flow. As a result of these effects, oil-producing zones will flow and produce with minimized restrictions. For a constant pressure, the 60 cP oil will flow 3, 4 times the rate of hot water (Fripp et al., 2013).

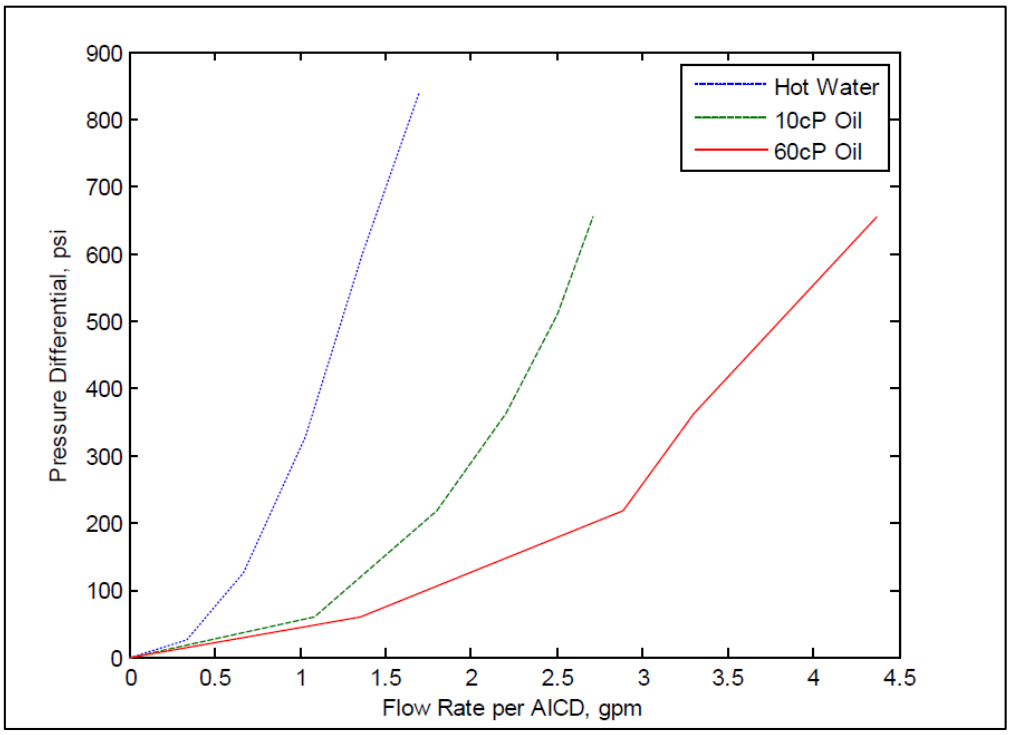

Figure 6: Measured flow through fluidic-diode type AICD, (Fripp et al., 2013)

2.3 Equalizer Select AICD

The Equalizer Select AICD from Baker Hughes, integrates a hybrid design with sequence of flow chambers aligned with immediate changes in directions and a long path to accomplish the particular pressure drop (Akbari et al., 2014). As the flows goes through channel into the next chamber the pressure is gradually reduced, as a result it reduces turbulence inductive jetting effects (7). Because of device geometry, plugging and erosion are not a problem.

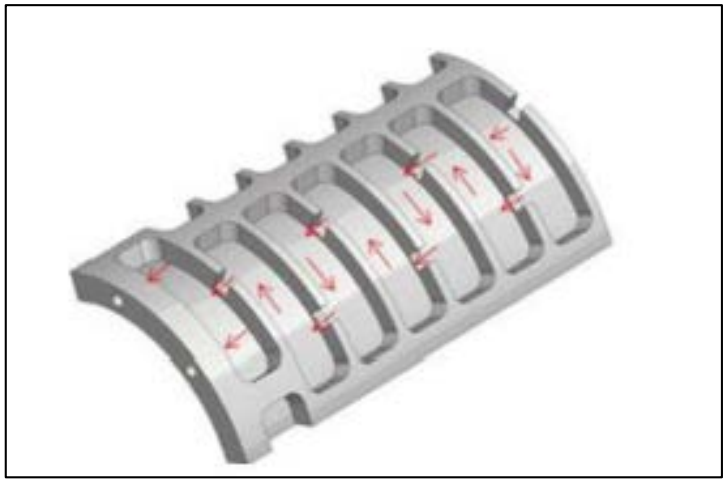

Figure 7: Flow Path through Equalizer Select, (Akbari et al., 2014)

The design enables flow control through a wide range of production rates, densities and oil viscosities during the well's life (Akbari et al., 2014). Therefore, it can be considered as an autonomous device because it has the ability to independently adjust the flow in dynamic conditions (Figure 8).

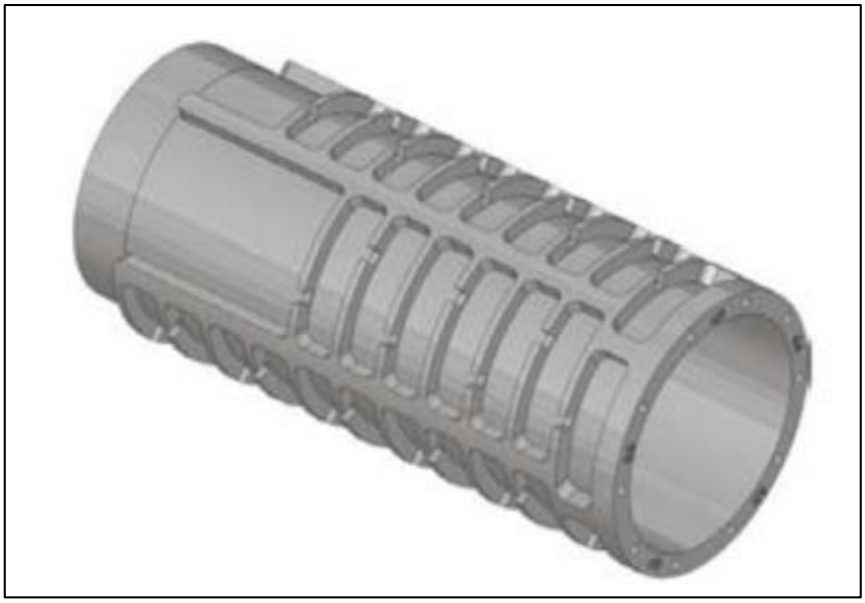

Figure 8: Autonomous Geometry of the Equalizer Select, (Akbari et al., 2014)

The independent flow resistance rating (FRR) of the device can be changed on the surface, prior to installation, therefore it can accomplish different production norms. FRR is term produced to analyze the amount of choking effect, and it is characterized as the pressure drop while water, with viscosity of 1 cP, flows through the device at the rate of 189 bpd (Akbari et al., 2014).

During oil production, Reynolds number has lower values, somewhere in the laminar region. When the water breakthrough happens, composition of the flowing fluid is changed, due to the increased volume of water which leads to the increase in Reynolds number, thereby increasing the pressure drop and choking effect (Banerjee et al., 2013).

In order to describe the performances of this device, pressure drop is expressed with the dimensionless pressure drop coefficient (K) which is a function of Reynolds number and device dimensions. The reason to do this, is to achieve as accurate as possible performances of the device, by combining pressure drops due to density and velocity in combination with a viscosity pressure drop, which are all included in (K). Figure 9 shows the relation between dimensionless pressure drop coefficient and Reynolds number for Equalizer Select AICD (Banerjee et al., 2013).

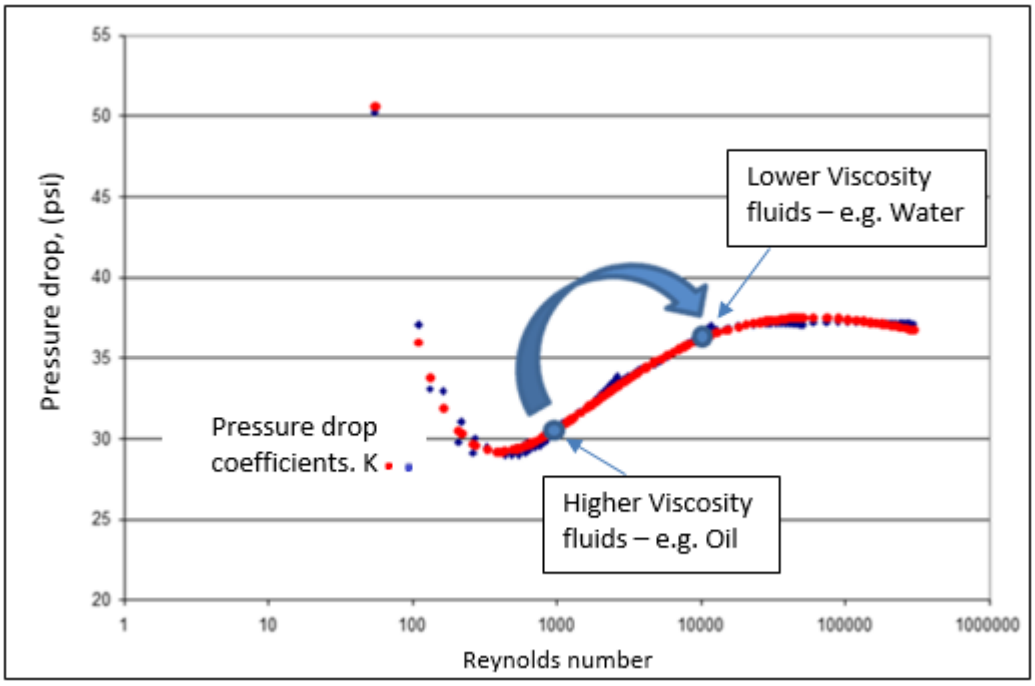

Figure 9: Relation between pressure drop coefficient and Reynolds number, (Banerjee et al., 2013)

From Figure 9 it can be observed that as the fluid flow goes from laminar flow regime (Re=1000) to a turbulent flow regime (Re=10000), the pressure drop/pressure drop coefficient increases (Banerjee et al., 2013).

2.4 Wormhole AICD

The third generation of Wormholes ICD is the Adaptable Inflow Control System (AICD) capable of self-adjustment depending on fluid rate, pressure and phase composition. Flow control is achieved due to design of the special valves and adjustment of the flowrate through them providing for the required valve activation (opening or closing) pressure drop at the preset flowrate (Delia et al., 2015). The device can be used efficiently in producing thin oil reservoir sections uniformly, through the long reach horizontal wells. It is able to react on abrupt increase in flow rate, due to the higher flowing ability of water and gas, therefore limiting the inflow in the breakthrough zones or even completely isolating them. In addition, besides it can be closed automatically, it can also be closed manually by increasing the drawdown or mechanically isolating wanted zones. Raising the wellhead pressure will open inflow in the complete well.

Figure 10 shows the simplest variation of the Wormhole AICD. The system is composed of throttle rings with predetermined hydraulic properties and valves with a permanent gate position (open or closed) (Delia et al., 2015). Valves are made to adapt to various AICD

requirements by choosing the right valve saddle cross-section and gate plate rigidity. Thereby valves properties are changed (opening and closing pressure drop) at the predetermined flowrate.

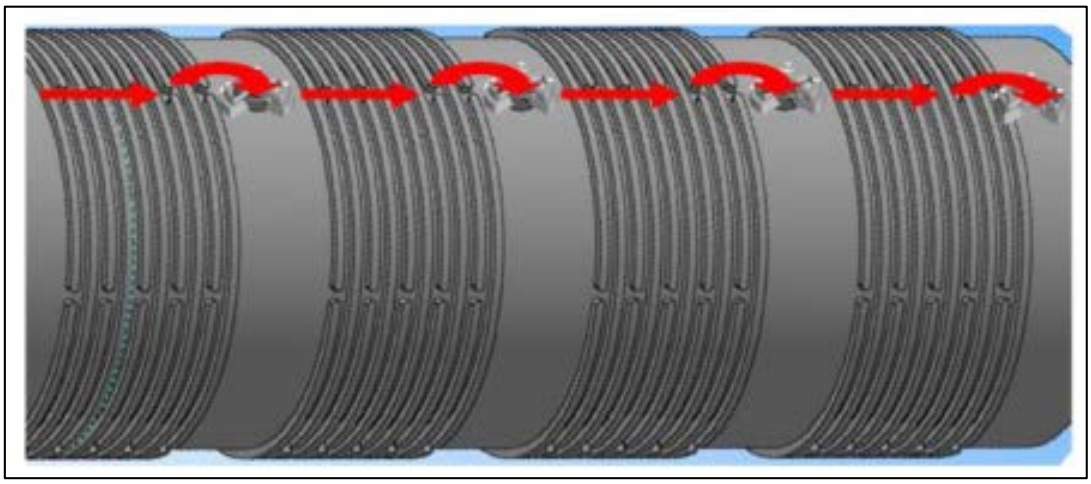

Figure 10: Schematic of Adaptable Flow Control System Operation, (Delia et al., 2015)

Figure 11 shows how the device reacts to the change of overall flowrate and the pressure drop in the system during testing. The sudden pressure rise and decreases of the flowrate are connected to the activation of the AICD valves (Delia et al., 2015).

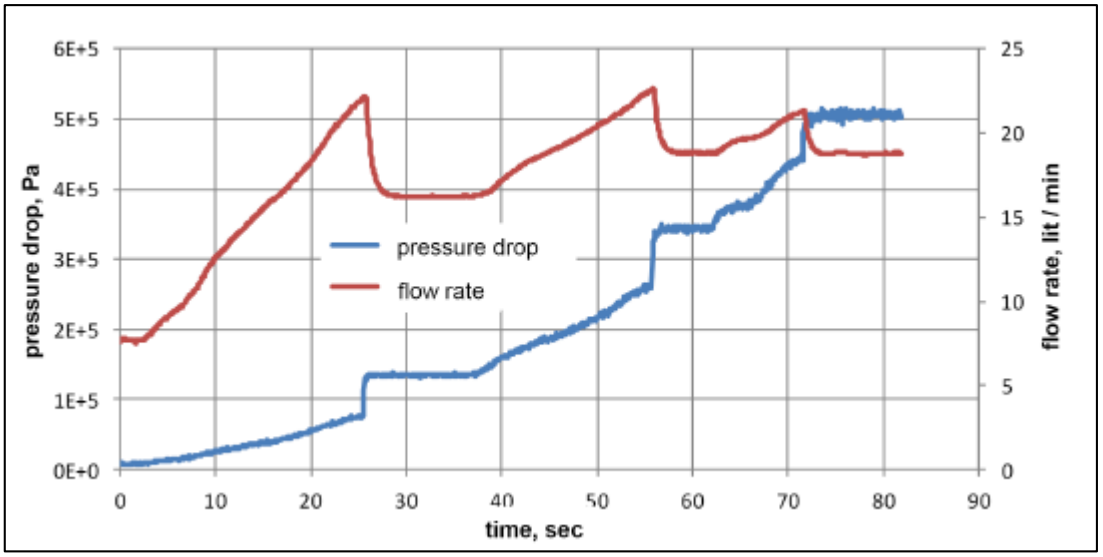

Figure 11: Pressure Drop with Flowrate in the System, (Delia et al., 2015)

2.5 Counterweight Floating-Flapper Valve

Counterweight Floating-Flapper Valve, developed by Baker Hughes, is designed in that way to passively choke the production through the screens and the production equipment when it detects the breakthrough of the gas in horizontal and highly-deviated wells. This is done by using the density-sensitive flapper type valve (Figure 12) in every screen joint in the production well. The device uses the Archimedes principle which states that every submerged solid will be exposed to the force equal to the weight of the fluid it displaces (Crow et al., 2006). The force will act on the center of gravity of the submerged solid. If the buoyancy force of the fluid is lower the force from the weight of the valve, it will sink and close. Otherwise, if buoyancy force is high enough to overcome the force form the weight of the valve, it will float and be in the open position.

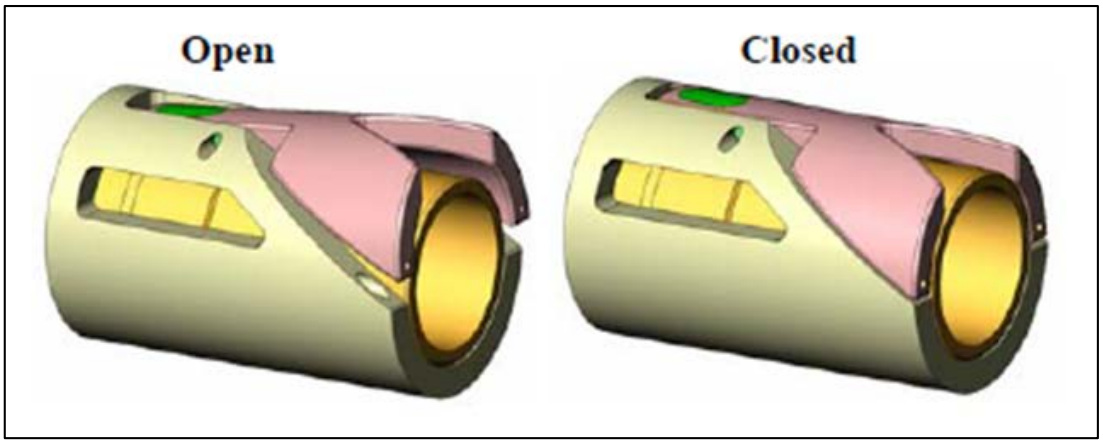

Figure 12: Floating flapper type valve, (Crow et al., 2006)

As the gas starts flowing into the particular part of the well, the density is decreased in that region, and the valve starts closing. After the oil front is reestablished in the mentioned area and the density increases, the valve will start to open, and continue the production of the oil (Crow et al., 2006).

The system allows the isolation, with open hole packers, and production from every screen joint independently. Therefore, it can prevent the gas coning problem in each section separately. The valve is totally autonomous and it doesn't require any connection and power from the surface. It is also important to mention, that as the valve is integral part of the screen sections it allows full bore production and access for intervention tools. Another important point to mention for this device, is that the inflow control part of the device is the regular ICD (Crow et al., 2006).

In order to make this design possible in terms of the usage of the industry available today,

the counterweight is introduced in the device design (Figure 13). With change of the counterweights mass, the device can be set for the particular type of the downhole conditions and fluid properties (Crow et al., 2006).

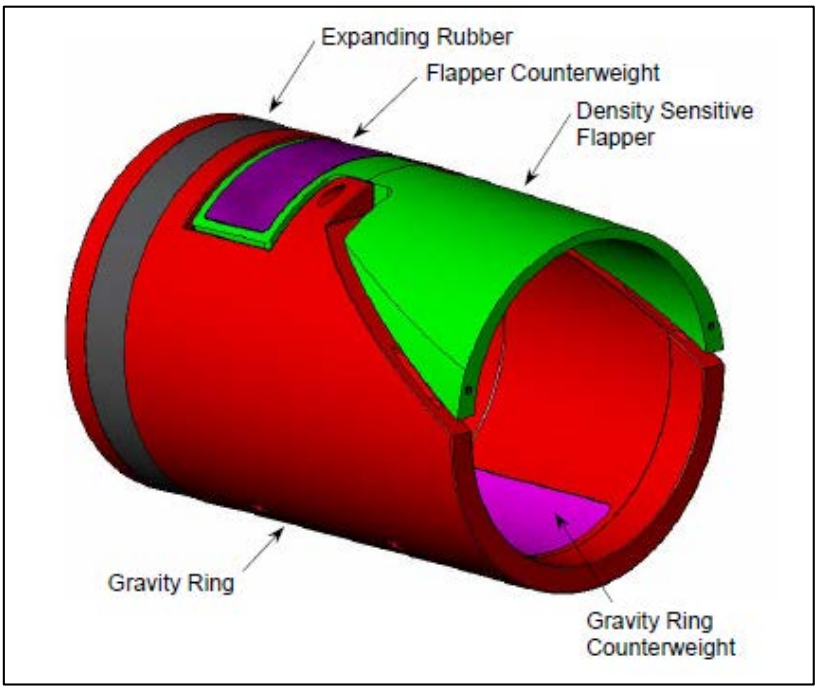

Figure 13: Counterweight Flapper Design, (Crow et al., 2006)

Figure 13 also shows the usage of the same counterweight design for the Gravity Ring. Purpose of the Gravity Ring is to orientate the device in the correct position, so it can function properly in the horizontal and highly-deviated wells. Orientation of the AICD device is of critical importance for its proper functionality. The floating flapper has to be on the top of the section, regardless the position of the screens installed. Roller bearings are used in the combination with the off-center Gravity Ring counterweight in order to position the device in the correct position in the well, regardless any debris or other downhole problems (Crow et al., 2006).

Another thing that is shown on Figure 13 is the Expanding Rubber element on the back of gravity ring, and its purpose is to isolate the gas influx by expanding the rubber element in the contact with hydrocarbons. It is designed in such way it allows the device to move freely in the well during installation, and to run all the necessary operations (sand face completion) before it expands completely and isolate the section. The AICD device also includes the bleed orifice which allows the slow bleed off of the accumulated gas, providing enough back pressure to force the production of oil from other sections of the well. If the gas is no longer present around the device section, the oil production will be

reestablished (Crow et al., 2006).

Inflow performance of the device is based on the ICD device system that is used in the completed well. The task of the device is to isolate the gas inflow when it occurs, and the inflow control is controlled by the ICD. In combination, these two systems, Floating Flapper Valve for isolating the gas influx and an ICD for controlling the inflow performance, can be referred as an AICD system (Crow et al., 2006).

2.6 Rate Controlled Production (RCP) Valve

The Rate Control Production (RCP) Valve is developed by Tendeka AS for Statoil AS primarily for Troll field production. RCP valve is completely autonomous and therefore it doesn't require any control or power (hydraulic or electric) from the surface. Properties and function of the RCP valve is based on the Bernoulli's principle. Figure 14 shows a profile picture of the RCP valve (Halvorsen et al., 2012).

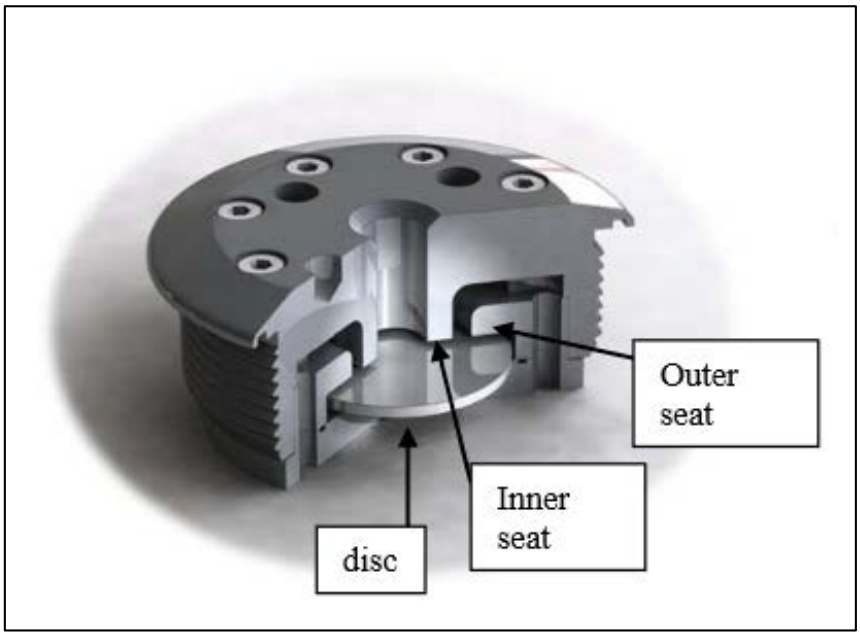

Figure 14: Statoil's RCP valve, profile picture, (Halvorsen et al., 2012)

The outer diameter of the RCP valve is usually 80 mm and the valve has only one moving part, the free floating disc inside the valve. Figure 15 shows schematic picture of the flow path through the valve marked by arrows. In this position of the movable disc, the valve allows maximum flow (Halvorsen et al., 2012).

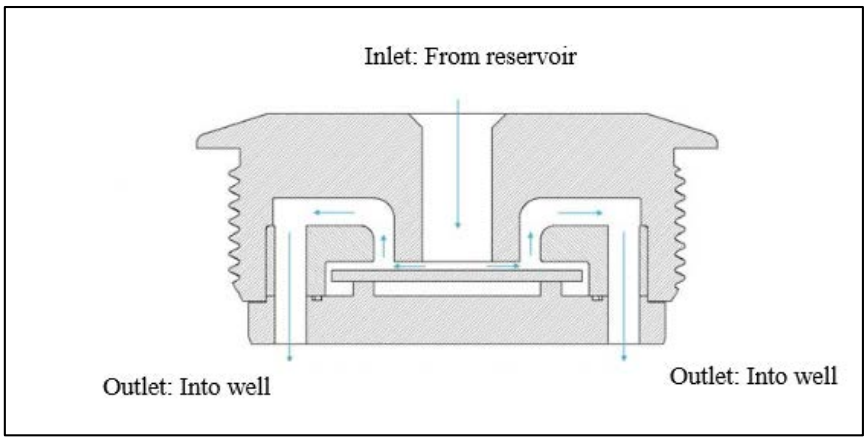

Figure 15: Schematic picture of the RCP valve, (Halvorsen et al., 2012)

The valve chokes the flow of fluids with low viscosity. When gas enters the valve and starts flowing through, the pressure on the top side of the disc shall be reduced, due to the high flowing speed of the gas (Bernoulli Effect). Therefore, the disc will move up, due to the reduced pressure on the top and pressure acting beneath the disc (stagnation pressure) which is higher, and the pressure difference will close the valve. Figure 16 shows how the fluids with different viscosities follow different streamlines through the valve. From that reason, the stagnation pressure will be much larger for gas flow compared to oil flow. Therefore, when gas is flowing the stagnation pressure will push the movable disc towards the seats and close it. This action will make the flow area smaller and choke the gas flow (Halvorsen et al., 2012).

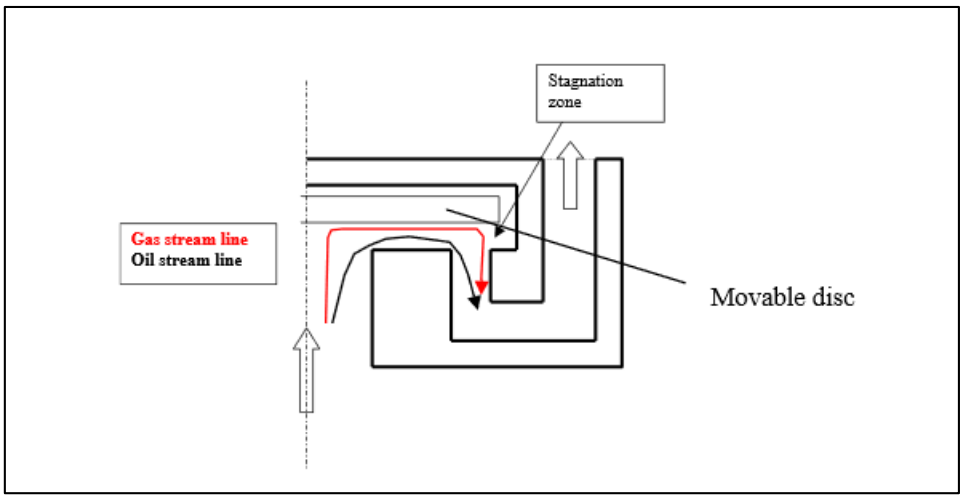

Figure 16: Sketch of the RCP valve with typical streamlines, (Halvorsen et al., 2012)

Figure 17 shows the situation of strong gas flow choking in a cross section of the valve together with pressure profiles. Pressure profile is sketched in AA' line. The pressure at the point A represents the pressure on the reservoir side, which is not necessarily the same

as the reservoir pressure (PR). The pressure acting from well side, between inner and outer seats is back pressure (PB). Pressure at point A' is stagnation pressure (Pst). As mentioned above, stagnation pressure will push the disc towards the seats and the resulting force between reservoir side and stagnation pressure will push the disc up, in closed position. When the valve closes, there is a metal to metal connection between the movable disc and the outer seat. It is important to ensure optimal gas choking. The contact between seat and disc maintains the stagnation pressure in the stagnation chamber, at least for a short period of time (Halvorsen et al., 2012). When the stagnation pressure in the stagnation chamber drops below the opening pressure of the valve, the force acting bellow the disc, becomes too low to hold the disc in closed position and the valve opens. Time period that takes the stagnation pressure to get back to the opening pressure of the valve is referred as an opening/closing frequency of the valve (Halvorsen et al., 2012).

Two pressure profiles sketched, represent the isolation contact between the disc and the outer seat. The green curve shows one limiting situation which exists when the sealing is around the center of the inner seat and around the stagnation point at the outer seat. Whereas, the red curve shows other limiting situation, when the sealing is around outlet at both seats (inner and outer). Integration bellow both of the curves gives as a result the pressure force. The pressure profile that is optimal is the pressure represented by the red curve. To ensure this profile, cones at the inner and outer seat have been included, thus optimizing the gas choking effect (Halvorsen et al., 2012).

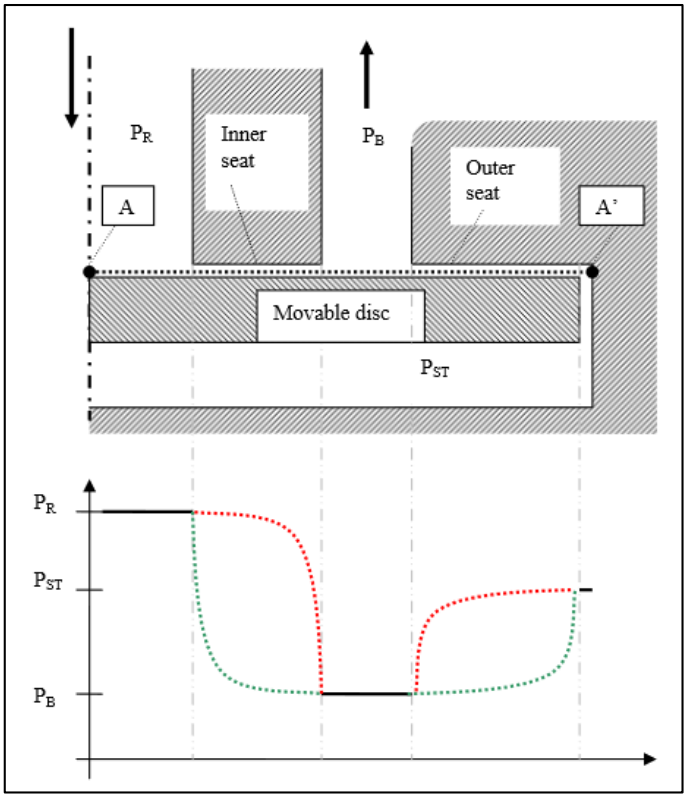

Figure 17: Cross section of valve and pressure profile at disc in closed position, (Halvorsen et al., 2012)

As the fluid with higher viscosity starts flowing through the valve, the friction pressure losses are higher. Because of that, the dynamic pressure recovery is also reduced. Therefore, the stagnation pressure will reduce, and the disc moves away from the inlet side and flow area and rate increase. Following this, heavier oils will flow with lower resistance then lighter oils. Nozzle or an orifice based fixed type device, will have different effect (Halvorsen et al., 2012).

Since the valve is viscosity controlled, it will choke gas flow in the light oil reservoir, and water flow in heavy oil reservoir.

Figure 18 shows performance curves for gas, water and heavy oil flowing through RCP valve (Halvorsen et al., 2012).

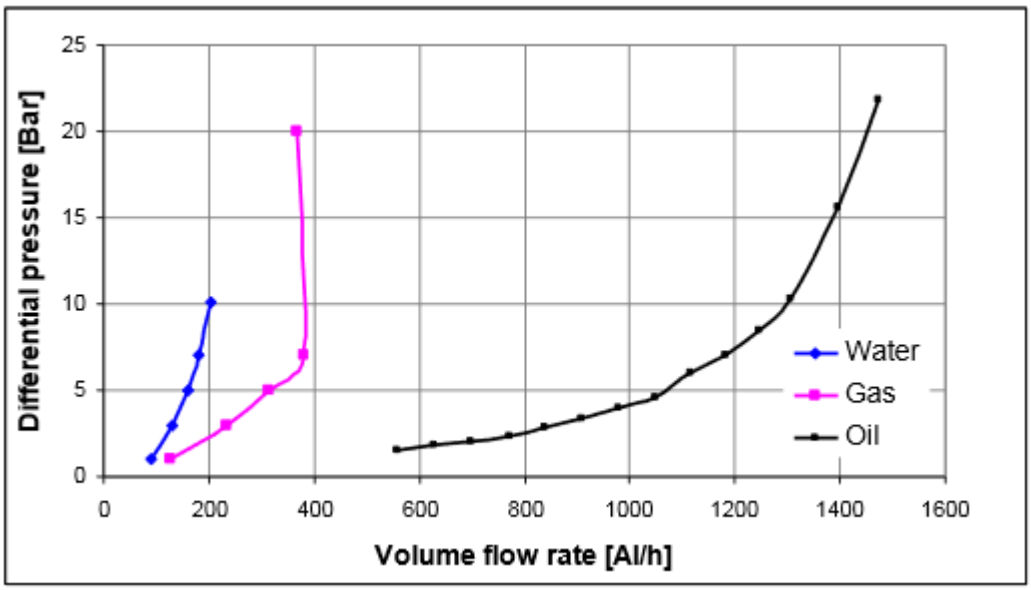

Figure 18: Volume flow of heavy oil, water and gas through RCP as a function of differential pressure, (Halvorsen et al., 2012)

2.7 Autonomous Inflow Control Valve (AICV)

Autonomous Inflow Control Valve (AICV) combines the properties of the AICD and ICV in one device. As all the others, AICV also does not require any control and connection to surface, it is completely autonomous. It is designed in that way that allows the flow of oil through it, with small restrictions, weather gas and water are almost completely stopped. Together with the devices mentioned above, it can be used in long reach horizontal wells. Purpose is to stop the breakthrough from one zones and in the same time continue producing oil from other zones without the breakthrough. The AICV is completely reversible, which means that whenever oil settles around the valve, it will start producing again (Aakre et al., 2014).

The principle that is used in AICV is based on disparity in the pressure drop between laminar and turbulent flow restrictors. Figure 19 shows simplified picture of the principle involved together with pressure profiles for different fluids (Aakre et al., 2014).

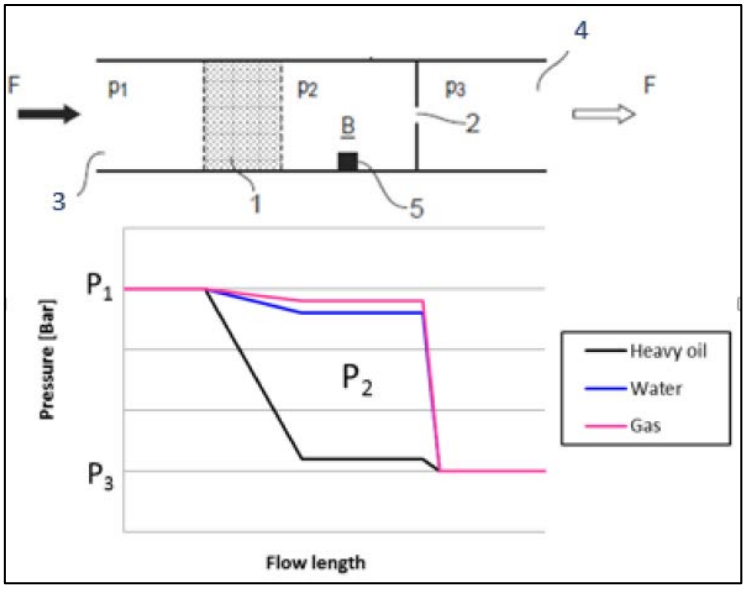

Figure 19: Combination of laminar and turbulent flow restrictors in series, (Aakre et al., 2014)

Referring to the Figure 19, the inlet from reservoir side is marked with number 3, whereas the outlet to the production equipment is marked with number 4. Pressure profile given in the same figure, shows different pressures at different points in the valve for heavy oil, gas and water. The valve is sensitive to fluid properties and flow rate, which are used to control the pressure in chamber B. The pressure in chamber B is controlling pressure for the valve. When the heavy oil with high viscosity if slowing through the restrictors, pressure drop in the chamber B is high, thus the piston will be in open position and produce oil. In contrary, when low viscous fluid is flowing through laminar restrictor, losses will be smaller. Therefore the pressure in the chamber B will be high which activates the piston up, and closes the valve (Aakre et al., 2014).

Figures 20 and 21 show the AICV in open and close position, respectively. The thin blue lines shows the pilot flow path, the thickest blue arrow presents the inlet of the main flow to the valve, and the two horizontal arrows show the outlet of the main flow to the base pipe. The thin blue line shown in the Figures, represents the outlet of the pilot flow (Aakre et al., 2014). The yellow piston is activated with pressure in chamber B, P2. Force F1 acts on the top of the piston, F1=A1*(P1-P3), whereas the force F2 act from the bottom of the piston, F2=A2*(P2-P3). These difference between these two forces give the resulting force which controls the valve. If the resulting force (F1-F2) is positive the valve will be in open position. Whereas, if the resulting force is negative valve will close. Since the pressure P1 comes from reservoir side, it is regularly higher then pressure in the chamber B, behind the piston P2. The controlling parameters of the valve are based on ratio between areas A1

and A2. Because the pressure P1 is higher than pressure P2, the area A2 has to be larger that area A1. These areas are the design parameters for the valve, dependent on the properties of the fluids (Aakre et al., 2014).

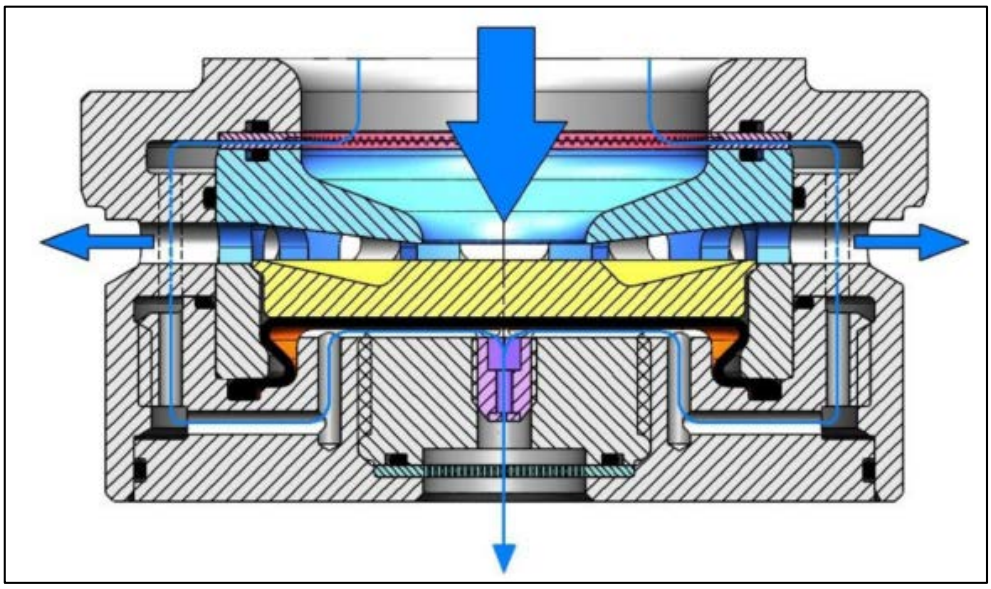

Figure 20: AICV in open position, (Aakre et al., 2013)

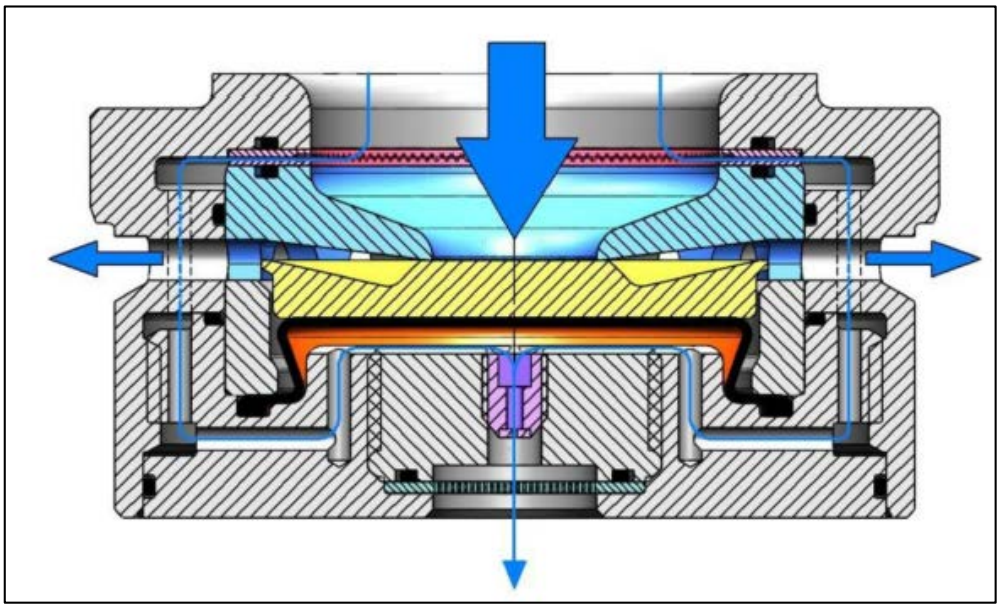

Figure 21: AICV in close position, (Aakre et al., 2013)

Figure 22 shows a comparison of performances between ICD and AICV devices for oil and gas.

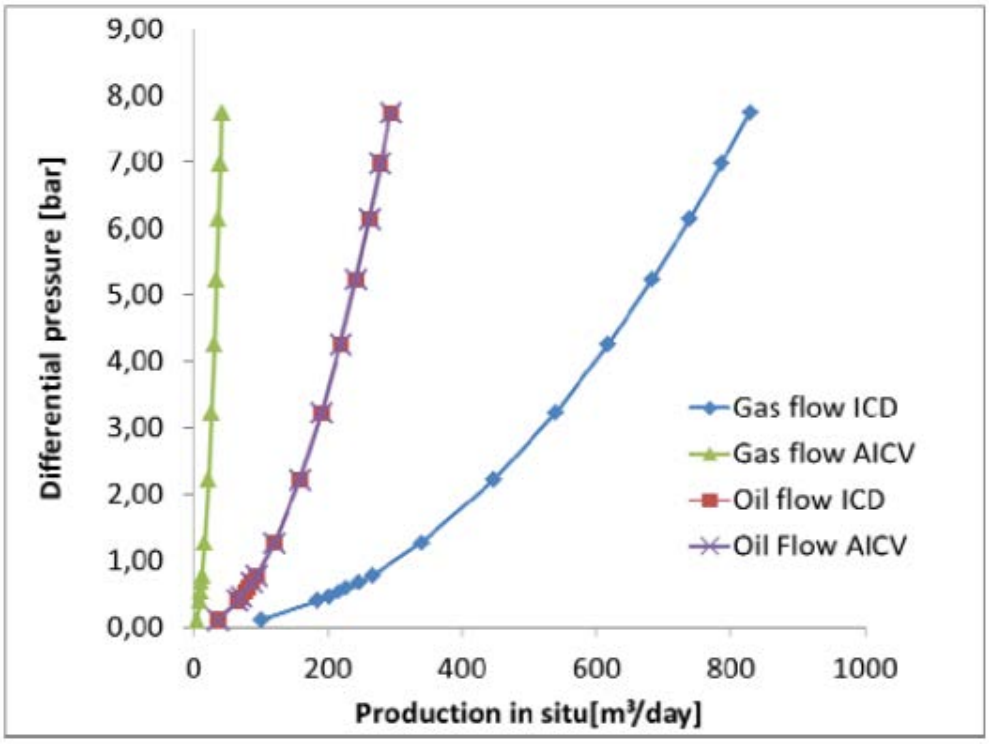

Figure 22: Oil and gas flow through the ICD and AICV versus differential pressure, (Aakre et al., 2013)

3 Methodology

Because lack of the design data for each AICD, different approach is going to be used in order to determine performance relations, except for the AFD valve and Wormhole AICD. The process will involve using the preexisted experimental performance curves for different types of fluids, and creating the set of constants and exponents from them, to describe AICD performances. The form of logarithmic expression (1) that is going to be used is (Aadnoy, 2010):

$$\Delta P = C * q^n \quad (1)$$

Where: ΔP – pressure drop across the AICD body (bar);

q – flow rate (m^3/d);

C – proportionality constant;

n – flow rate exponent.

After collecting pressure drop – flow rate relations from experimental data sets, for every AICD, using the equation (1), proportionality constants (C) and flow rate exponents (n) will be calculated.

In order to calculate proportionality constants (C) and flow rate exponents (n) for flow of one type of fluid though AICD, one experimental data set for that fluid and AICD is going to be used. Combination of two sets of values for pressure drop (ΔP) and flow rate (q) are inserted in the equation (1), in order to generate system of two equations (2, 3), with two unknowns.

$$\Delta P_1 = C * q_1^n \quad (2)$$

And,

$$\Delta P_2 = C * q_2^n \quad (3)$$

By applying the logarithmic function – ln, on both of the equations (2, 3) and subtracting them, flow rate exponent (n) can be calculated (4, 5).

$$\ln\left({}^{\Delta P_1}/_{\Delta P_2}\right) = n * \ln\left({}^{q_1}/_{q_2}\right) \quad (4)$$

Following,

$$n = \frac{\ln\left({}^{\Delta P_1}/_{\Delta P_2}\right)}{\ln\left({}^{q_1}/_{q_2}\right)} \quad (5)$$

With known flow rate exponent (n) it is simple to find proportionality constant (C), just by inputting (n) in any of the equations (2, 3).

3.1 Performance Data Analysis (C, n)

The idea is to create sets of proportionality constants (C), and flow rate exponents (n) for every AICD, which can be used to describe their performances for particular fluid types. One limitation of this method, is that evaluated sets of constants and exponents are only valid for the particular fluid types and conditions, and one system of units. In this thesis, the SI system of units is used. Since the goal of this thesis is to compare different types of AICDs and their performances in similar conditions, this method is acceptable.

Flow rate exponent (n) is connected with the flow area of the device, and therefore the velocity of the flowing fluid. Every AICD has its own flow rate exponent (n), independent of the flowing fluid type (water, oil or gas). Higher values for flow rate exponent (n) represent a smaller flow area, and therefore the increases in velocity. Lower values of the flow rate exponent (n) represent larger flow areas and the decreases in velocity. For the pure laminar flow, where the velocity is lower due to the higher viscosity of the fluid, value of the flow rate exponent is equal to 1. For the ICD – nozzle, where the flow has higher velocity, and it is in turbulent flow regime, the value of the flow rate exponent is equal to 2. For the purpose of the work in this thesis, the starting value of the flow rate exponent will be 2, as it is in the ICD – nozzle. Since the AICDs are going to be compared with the regular ICD – nozzle, this will show the differences in the flow areas between them. Values for the flow rate exponent (n) that are higher than 2, shows higher pressure drop progression, and therefore steeper curves in the pressure drop – flow rate diagrams.

Proportionality constant (C) is expected to show AICDs behavior with the change of fluid properties (viscosity, density). How the viscosity or density of the flowing fluid changes, the proportionality constant (C) should change. For the increase in viscosity of the flowing fluid the proportionality constant (C) should decrease. As for the density effect, when the density of the flowing fluid increases, the proportionality constant (C) is also increasing. The smaller the value for proportionality constant (C), the choking effect is reduced, and vice versa.

After parameters proportionality constants (C), and flow rate exponents (n) are calculated for every AICD, they will be used to describe the performances of each of them. Also, this data is going to be used to compare them in between, in order to find out and discuss the differences in performance characteristics.

4 Principles and Performances of AICDs

The idea behind this chapter is to evaluate performance characteristics and principles of the AICDs listed in the previous chapter. Method for describing the AICDs performance characteristics is described in the Methodology chapter of this thesis.

Firstly, the performance and principle of the regular nozzle type ICD will be evaluated and presented, and afterwards AICDs will be also evaluated and compared with the ICD. Therefore, the comparison between passive and active autonomous inflow control devices will be covered, in order to check the differences between them.

All of the available AICDs are based and developed on more or less similar principles of fluid mechanics. The main principles used in their development are based on Bernoulli's principle and Poiseuille's Law. Bernoulli's principle is used for evaluating of flow performances for turbulent (density controlled) regimes. Poiseuille's Law is used for evaluating of flow performances for laminar (viscosity controlled) regimes. Some types mentioned are also controlled by the Buoyancy effect, or they are pressure sensitive in addition to other properties.

4.1 ICD nozzle Principle

The principle of an ICD is related to generating pressure drop across the ICD flow area following the Bernoulli's equation. Since the flow across an ICD is in the turbulent regime because of the higher flowing velocity, pressure drop is controlled by the density of the flowing fluid. Viscosity effect can be neglected.

In order to apply the Bernoulli's equation to describe the pressure drop through an ICD nozzle, some assumptions have to be made (Lauritzen & Martiniussen, 2011):

- Flow has to be steady and inviscid;
- Flow has to be assumed horizontal;
- Constant density;
- Neglect friction losses.

Following above mentioned assumptions, the Bernoulli's pressure drop equation (6) for a nozzle can be written in the following form:

$$\Delta P = \frac{\rho * v^2}{2 * Cd^2} \alpha\ \rho v^2 \ldots\ldots\ldots\ldots\ldots\ldots\ldots\ldots\ldots\ldots\ldots\ldots\ldots\ldots\ldots\ldots (6)$$

Where: ρ – fluid density (kg/m^3);

v – fluid velocity (m/s);

Cd – discharge coefficient.

Discharge coefficient is dependent on ICD design, it is usually given by the manufacturer of the device. In these calculations, constant discharge coefficient of 0.91 is assumed.

The final look of the equation (7) that is going to be used for describing the ICD performance, after the implementation of fluid flow rate (q) and surface area of the nozzle (A), inside the velocity parameter is:

$$\Delta P = \frac{8 * \rho * q^2}{Cd^2 * d^4 * \pi^2} \ldots\ldots\ldots\ldots\ldots\ldots\ldots\ldots\ldots\ldots\ldots\ldots\ldots\ldots\ldots\ldots (7)$$

Where: q – flow rate (m^3/d);

d – diameter of the nozzle (mm).

4.1.1 ICD nozzle Performance

Performance curves of an ICD nozzle, (Figure 23) are calculated using the equation (7). ICD is tested on the flow of water, oil and gas.

Fluids used for performance testing:

- Water – Density 993 kg/m^3, viscosity 1 cP;
- Oil – Density 849 kg/m^3, viscosity 10 cP;
- Gas – Density 103 kg/m^3, viscosity 0.02 cP.

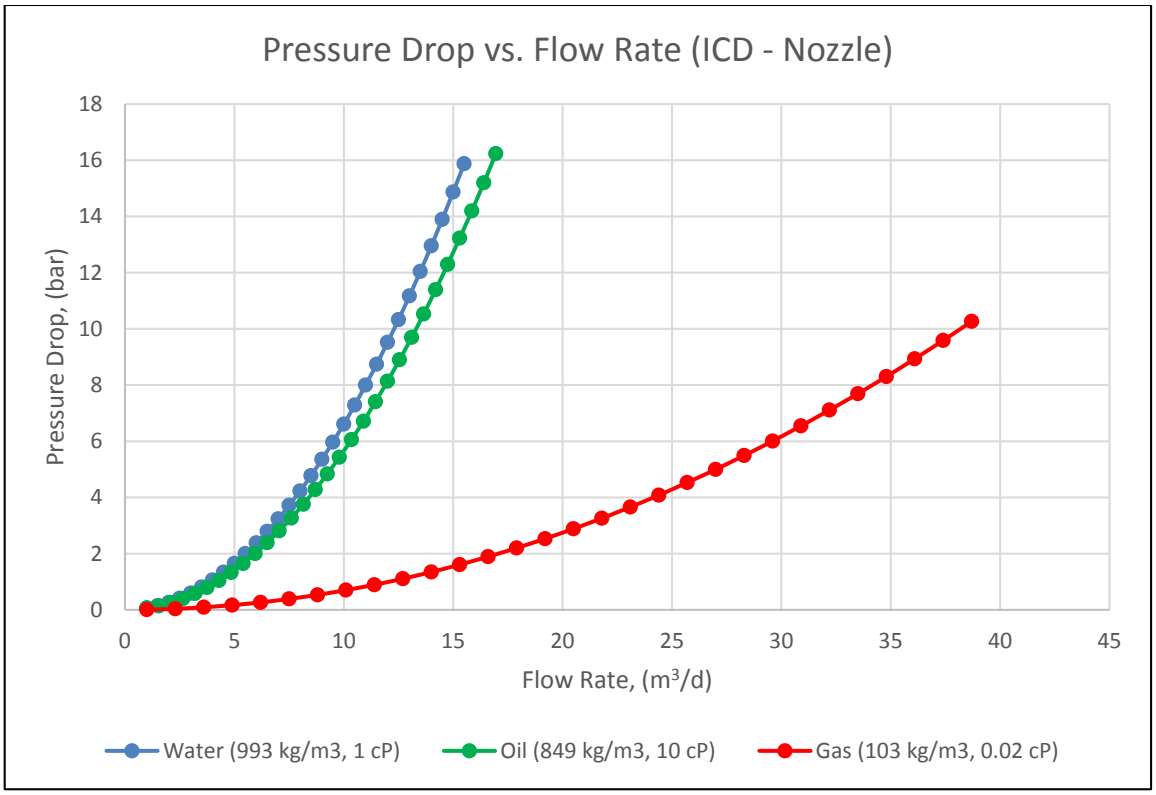

Figure 23: Performance curves for ICD nozzle, pressure drop dependence on flow rate

Figure 23 shows the performance of an ICD nozzle, and its main weakness. The regular nozzle ICD can choke the production, and slow down the occurrence of an early breakthrough of unwanted fluids (water or gas). Since it is a passive device, when the breakthrough occurs, ICD nozzle is not an adequate solution. ICD is not capable to provide additional choking effect when the content of water or gas increase. Curves on (Figure 23), for water and oil shows the small pressure drop difference between water and oil flow, and considerably smaller pressure drop for gas flow.

Performance data calculated from the input data, and performance curves in Figure 23, are presented in table 1 bellow.

Table 1: Performance data (C, n), for ICD - nozzle

	Proportionality Constant (C)	Flow Rate Exponent (n)
Gas (103 kg/m^3, 0.02 cP)	0.0069	2
Oil (849 kg/m^3, 10 cP)	0.0565	2
Water (993 kg/m^3, 1 cP)	0.0661	2

Looking at the data from table 1, it can be concluded that the flow rate exponent is equal to 2 (n=2), which is also shown in the equation 6 above, from the squared velocity term. As for the proportionality constant (C), it is clear that how the value for (C) is increased together with the increase in the density, the choking effect is increased going from gas, oil to water, respectively.

4.2 AFD Principles

AFD valve is a flow controller type of valve. It operates in that way it provides a constant flow rate independent from reservoir pressure drop. As explained in the chapter 2 of this thesis, AFD valve is based on two principles. The first principle is “hydraulic feedback principle”, for regulating the flow rate. Next one is Bernoulli’s principle (equation 8) which explains the pressure drop though the AFD.

The valve consists of valve body, moving piston and a spring, with a known spring constant K (Figure 24). When the reservoir pressure (P1) reaches the valve, it acts on the top part of the piston (larger area), and the bottom part of the piston where the spring is located (smaller area). The difference between these two forces, added to the constant spring force, regulates the opening of the valve, and therefore constant flow rate (hydraulic feedback principle). Pressure (P2) is well side pressure, and it is controlled by the Bernoulli’s principle, as for the pressure drop through the regular ICD – nozzle.

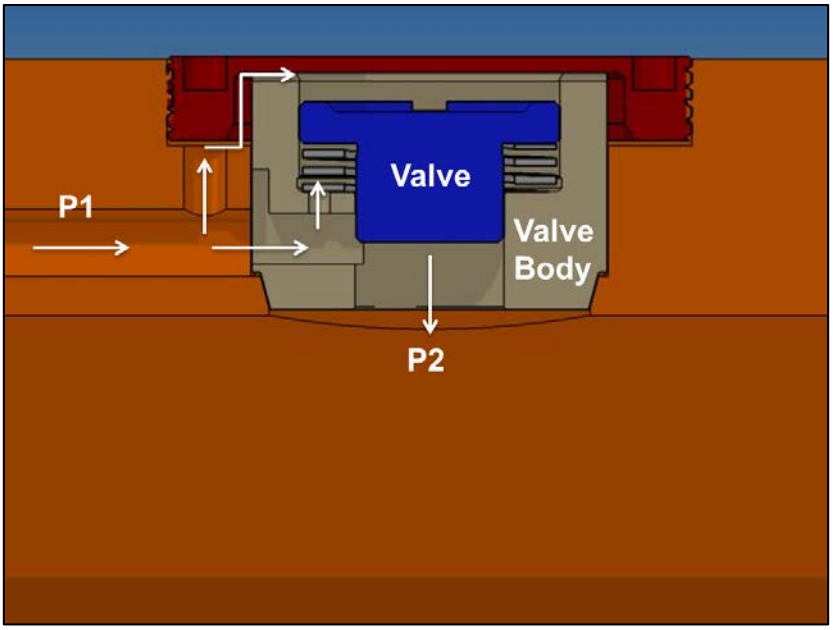

Figure 24: AFD valve configuration, (Bowen & Aadnoy, 2014)

Pressure drop based on Bernoulli's principle is shown in the equation (8):

$$P_1 + \frac{1}{2}\rho v_1^2 + \Delta P_{friction\ loss} = P_2 + \frac{1}{2}\rho v_2^2 \ldots\ldots\ldots\ldots\ldots\ldots\ldots\ldots\ldots\ldots (8)$$

Where: P_1 – reservoir pressure;

P_2 – well side pressure;

$\frac{1}{2}\rho v^2$ – dynamic flow pressure;

$\Delta P_{\text{friction loss}}$ – frictional pressure loss along the streamline.

4.2.1 AFD Performance

By analyzing the experimental data from (Bowen & Aadnoy, 2014), performance characteristics of the device have been tested. Since the device is different compared to the other AICDs, method described in the Methodology chapter, cannot be applied here.

Fluids used for performance testing:

- Oil: density 849 kg/m^3, viscosity 5 cP;
- Oil: density 890 kg/m^3, viscosity 121 cP.

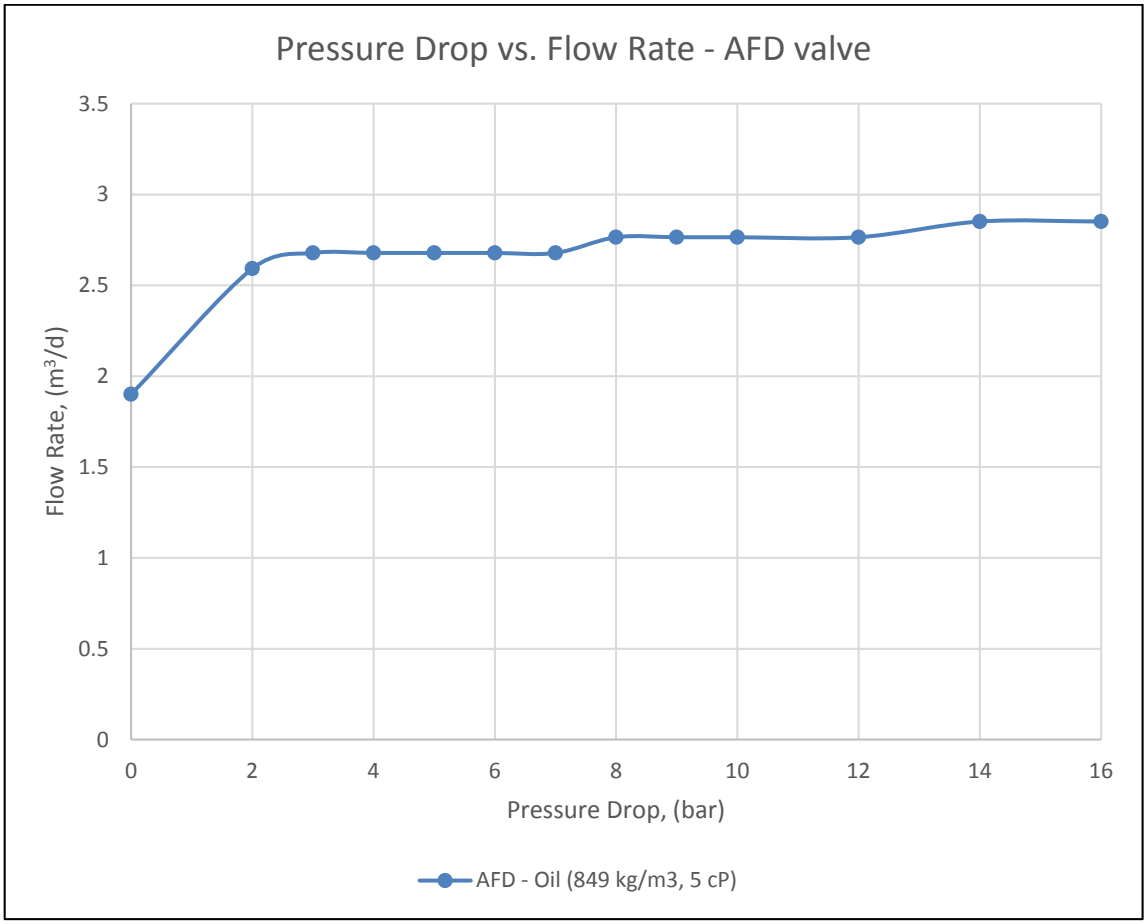

Figure 25: Performance curve for flow of oil (849 kg/m^3, 5 cP) through AFD valve, pressure drop dependence of fluid flow, (Bowen & Aadnoy, 2014)

Figure 25 shows the main property of AFD valve. As the flowing pressure changes, the pressure drop remains fairly constant.

The device has also been tested for the flow of oil with these properties (density 890 kg/m^3, viscosity 121 cP).

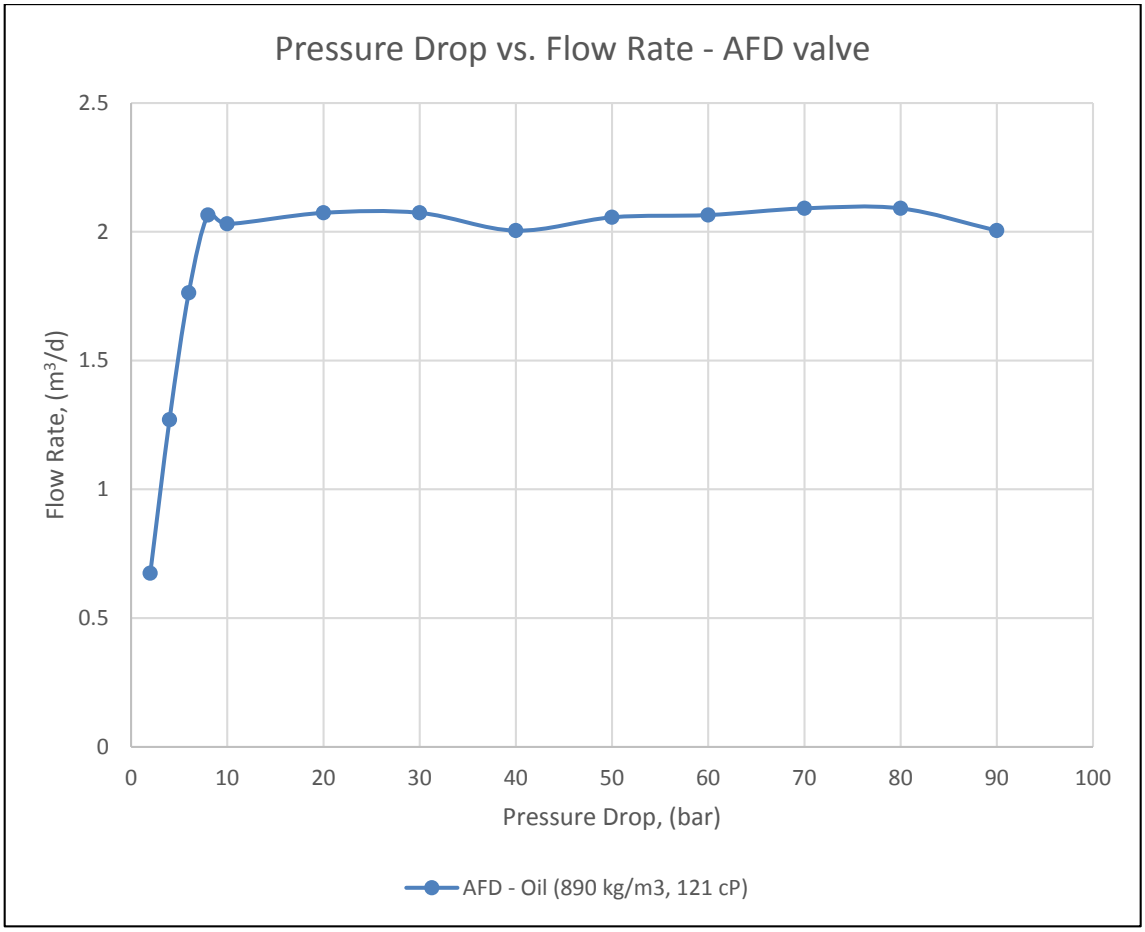

Figure 26: Performance curve for flow of oil (890 kg/m^3, 121 cP) through AFD valve, pressure drop dependence of fluid flow, (Bowen & Aadnoy, 2014)

Figure 26 shows the same performance as the previous one, the flow rate remains fairly constant through the pressure drop for the flow of heavier oil.

4.2.1.1 AFD valve vs. ICD Performance Comparison

Both devices were tested on the flow of oil, with the same properties.

Fluids used in performance testing:

- Oil: density 849 kg/m^3, viscosity 5 cP;
- Oil: density 890 kg/m^3, viscosity 121 cP.

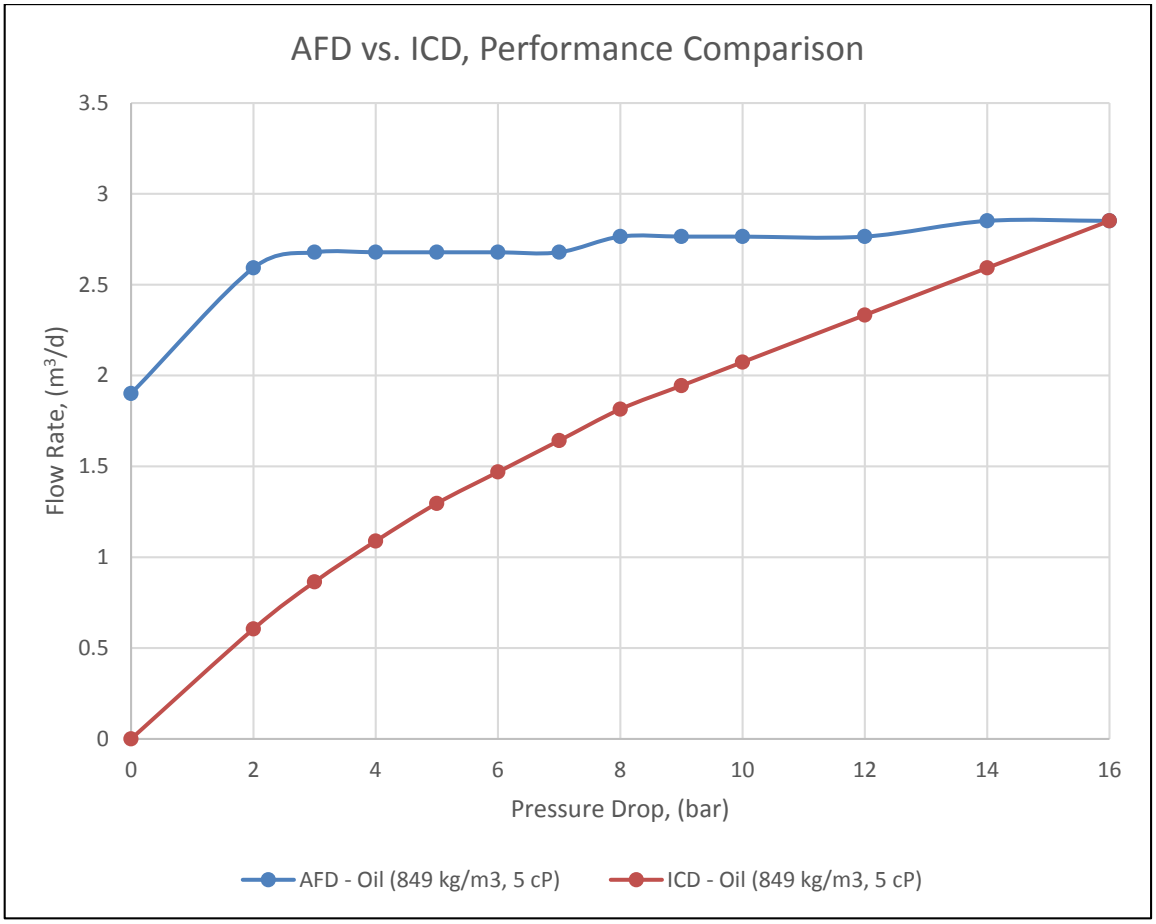

Figure 27: Comparison between flow of light oil through AFD and ICD – nozzle, (Bowen & Aadnoy, 2014)

Figure 27 shows, the main difference between AFD and ICD. As the pressure drop decreases fluid flow remains fairly constant for AFD, compared to the flow rate drop for the ICD. At the right end of the AFD curve, Bernoulli's effect can be seen. Where pressure drop – flow rate correlation follows the ICD trend line, up to some point of pressure drop.

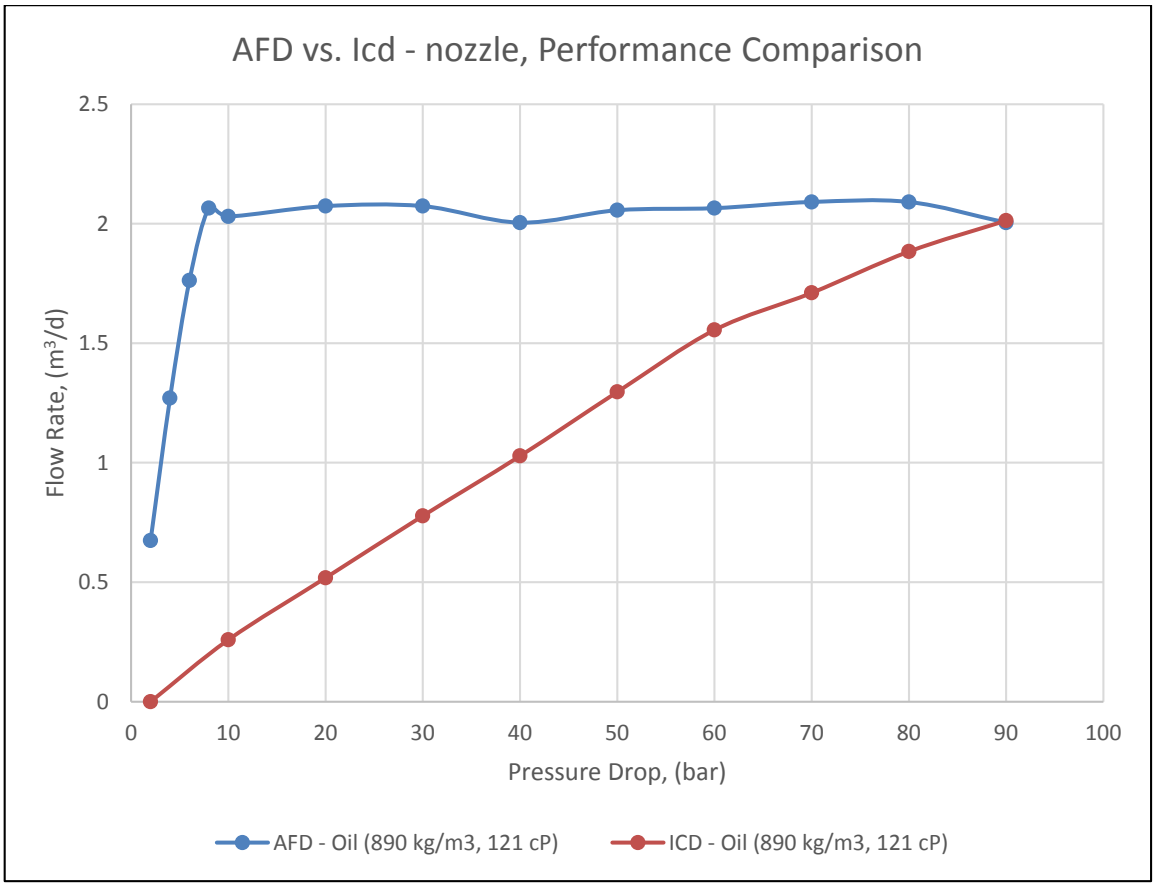

Figure 28: Comparison between flow of heavy oil through AFD and ICD – nozzle, (Bowen & Aadnoy, 2014)

Figure 28 shows comparison between flow of heavy oil (890 kg/m^3, 121 cP) through AFD and ICD – nozzle. The same trend line is present as for the previous test results for lighter oil (5 cP).

4.3 EquiFlow AICD Principles

EquiFlow AICD is mainly based and controlled with the viscosity of the flowing fluid. As explained in the chapter 2, fluids with lower viscosities (water or/and gas) will take the longer (tangential) path through the device and start spinning in the vortex (Figure 29). Thus, the angular momentum of the flowing fluid will be higher due to higher fluid velocity, as well as drag forces, which will increase the pressure drop. This will additionally choke the water or gas production zones, and allow normal production from oil producing zones.

Fluids with higher viscosities (oil) will experience the opposite effect. Viscous forces will pull the fluid flow between tangential and radial pathways. Therefore balancing the angular

momentum inside AICD and forcing fluid to take more direct path through the AICD with lower pressure drop (Figure 29) (Least, Greci, Wilemon, et al., 2013).

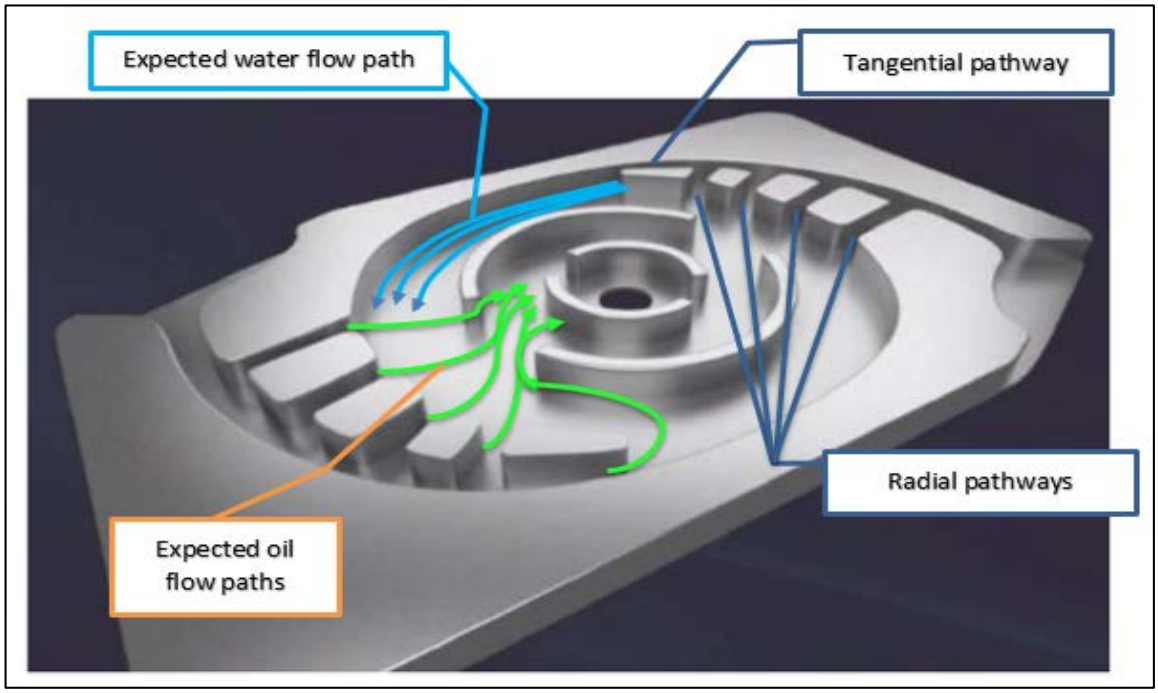

Figure 29: Tangential and radial pathways in EquiFlow, (Greci et al., 2014)

EquiFlow AICD, during normal production, provides the similar choking effect as the regular ICD, in order to prevent the occurrence of an early breakthrough.

4.3.1 EquiFlow AICD Performance

After analyzing experimental data and performance curves of EquiFlow AICD (Least, Greci, Wilemon, et al., 2013), and applying method described in the Methodology chapter of this thesis, following results are gathered.

Fluids used for performance testing:

- Water: density 993 kg/m^3, viscosity 1 cP;
- Oil: density 845 kg/m^3, viscosity 3 cP;
- Oil: density 849 kg/m^3, viscosity 10 cP;
- Oil: density 849 kg/m^3, viscosity 50 cP;
- Oil: density 856 kg/m^3, viscosity 76 cP.

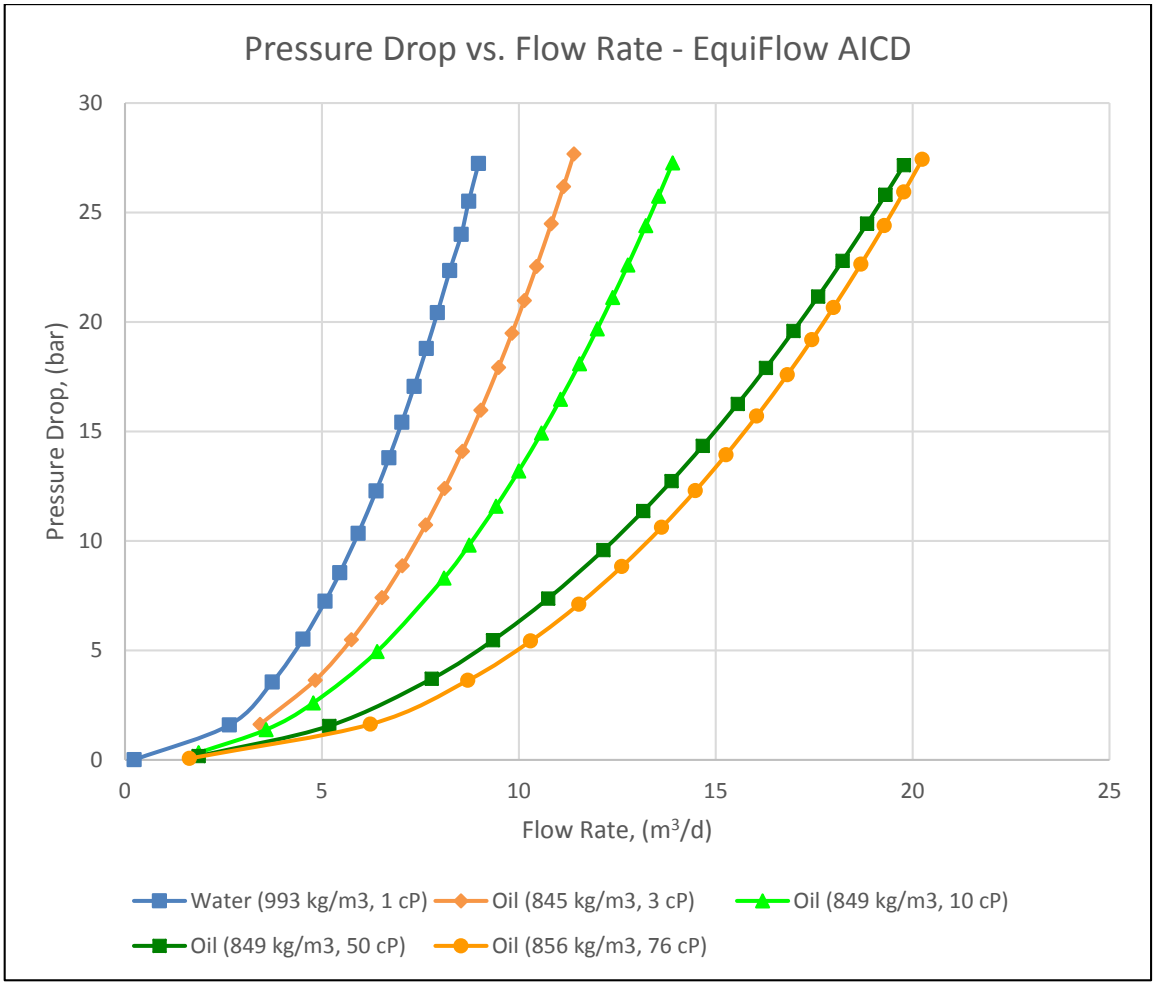

Figure 30: Performance curves for EquiFlow AICD, pressure drop dependence of fluid flow

Figure 30, shows the performance of EquiFlow AICD for flow of water, and four different types of oils, with different properties. Water as less viscous fluid, shows the quickest pressure drop progression, at smaller flow rates, compared to oil. Four types of oils, have shown a trend line, where the pressure drop progression decreases with an increase in flow rate, going from lower to higher viscosity oils, respectively.

One drawback of EquiFlow device, since it is viscosity sensitive, is the combination of water and light oil in the producing reservoir. The viscosities of light oil and water are similar, and for that reason, EquiFlow is not capable to choke water more than oil. Opposite, when reservoir fluids are the combination of heavier oils and water, EquiFlow can perform in its optimum range.

Gas flow is not included in this performance curve diagram (Figure 30) because the lack of the experimental the data.

Performance data calculated based on the performance curve on Figure 30, and the experimental data behind it, are presented in table 2.

Table 2: Performance data (C, n), for EquiFlow AICD

	Proportionality Constant (C)	Flow Rate Exponent (n)
Water (993 kg/m^3, 1 cP)	0.1646	2.3275
Oil (845 kg/m^3, 3 cP)	0.0884	2.3612
Oil (849 kg/m^3, 10 cP)	0.0835	2.1989
Oil (849 kg/m^3, 50 cP)	0.0461	2.1379
Oil (856 kg/m^3, 76 cP)	0.0203	2.3965

If we analyze the data for flow rate exponent (n) from table 2, it can be seen that the average flow rate exponent, including water and oil flow is around 2.3 (n=2.3). Looking at the results for proportionality constant (C), the choking effect is increasing with the increase in the proportionality constant (C), along with the decrease of the fluid viscosity.

EquiFlow AICD is built for various ranges of viscosities, depending on the fluid properties, especially viscosity ranges. The EquiFlow AICD type which performances have been analyzed in this thesis, is for low to medium range viscosities. But all the other types for higher viscosities function on the same principle, with very similar performance curves.

4.3.1.1 EquiFlow vs. ICD Performance Comparison

Here, performance characteristics of EquiFlow AICD are compared with ICD – nozzle performance. Fluids used for performance testing are the same, in both cases.

Fluids used for performance testing:

- Water: density 993 kg/m^3, viscosity 1 cP;
- Oil: density 845 kg/m^3, viscosity 3 cP;
- Oil: density 856 kg/m^3, viscosity 76 cP.

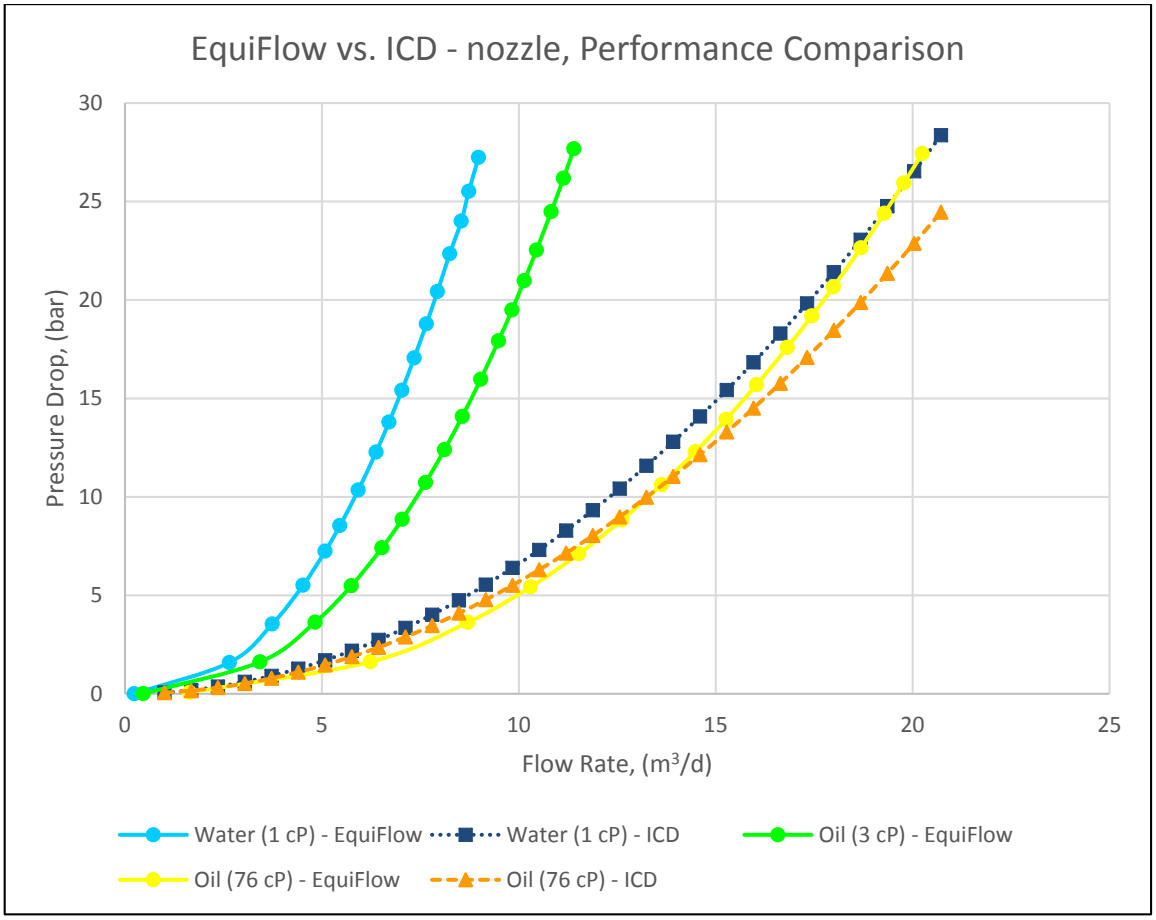

Figure 31: Comparison between EquiFlow and ICD - nozzle performance characteristics

Analyzing Figure 31, it shows the difference in performance characteristics of EquiFlow AICD and ICD – nozzle. Fluids marked with slotted dark blue and orange color, represent flow through ICD. Fluids marked with light blue, green and yellow color represent flow through EquiFlow AICD.

Comparing flow of water (993 kg/m^3, 1 cP), marked with blue colors on Figure 31, it shows large differences in choking effect of EquiFlow and ICD – nozzle. Pressure drop progression is much higher with the increase in flow rate for EquiFlow AICD than it is for the ICD – nozzle. EquiFlow AICD shows a wide gap in choking effect of water and oil, compared to the ICD – nozzle. This shows the selectivity property of EquiFlow AICD, depending on the fluid properties (viscosity).

Both ICD nozzle and EquiFlow AICD show almost the same flow control capability to choke oil production, in order to prevent early breakthrough of unwanted fluids.

Looking at the pressure drop curves for oil (76 cP), the flow rate exponent difference between EquiFlow and ICD can be seen. For ICD – nozzle is flow rate exponent is equal to 2 (n=2), and for EquiFlow is around 2.3 (n=2.3).

4.4 Equalizer Select AICD Principles

The Equalizer Select AICD, can be described as an autonomous Passive Inflow Control Device (PICD). It has a hybrid – geometry , which combines the frictional losses of fluid flow through a baffle with pressure drop through a series of restrictors in the same flow (G. A. Garcia et al., 2010; L. Garcia et al., 2009). This type of hybrid - geometry device pressure drop is independent of viscosity of the fluid, in wide range from 8 cP through 900 cP (Banerjee et al., 2013). As mentioned in in the chapter 2, Equalizer Select AICD can be set with a variety of different Flow Resistance Ratings (FRR) (table 3).

Table 3: Available FRR settings, (Abdelfattah et al., 2012)

	Pressure Loss Magnitude			
	Low	→		High
FRR	0.8	1.6	3.2	6.4

Every flow path through the device has its own FRR value, as shown in table 3 above. Flow path (Figure 32) can be set prior to installation, depending on accessible field data and fluid properties.

Figure 32: Flow paths through Equalizer Select AICD, (Abdelfattah et al., 2012)

Mathematically, the performance of the device can be best described using the equation (9).

$$\Delta P = K * \rho * \left(\frac{q^2}{2 * g * 144}\right) * \frac{1}{A^2} \quad \ldots\ldots\ldots\ldots\ldots\ldots\ldots\ldots\ldots\ldots\ldots\ldots\ldots (9)$$

Where: ΔP – pressure drop through the device;

K – pressure loss coefficient;

ρ – fluid density;

q – fluid flow rate;

g – gravity constant;

A – cross sectional flow area of the device.

Where K, describes the restriction through the device. The coefficient K changes the friction factor described by Reynolds and the pipe geometry/dimensions, for the frictional pressure drop in a tube. Nevertheless, the pressure loss coefficient is highly dependent on the flow geometry of the device and fluid properties itself.

4.4.1 Equalizer Select AICD Performance

Performance characteristics of Equalizer Select AICD are a bit different compared to the other AICD devices. As for the others, viscosity or density are the main driver parameters for their performance, for the Equalizer Select it is pressure loss coefficient K, which is a function of Reynolds number.

Fluids used for testing the performance characteristics of the device, have a wide range of viscosities, in order to show the viscosity insensitivity of the device. After analyzing the experimental data presented in (Akbari, 2014), following results are developed.

Fluids used for performance testing:

- Water: density 1100 kg/m^3, viscosity 0.85 cP;
- Oil: density 890 kg/m^3, viscosity 4 cP;
- Oil: density 890 kg/m^3, viscosity 18 cP;
- Oil: density 890 kg/m^3, viscosity 52 cP;
- Oil: density 890 kg/m^3, viscosity 82 cP;
- Oil: density 890 kg/m^3, viscosity 200 cP.

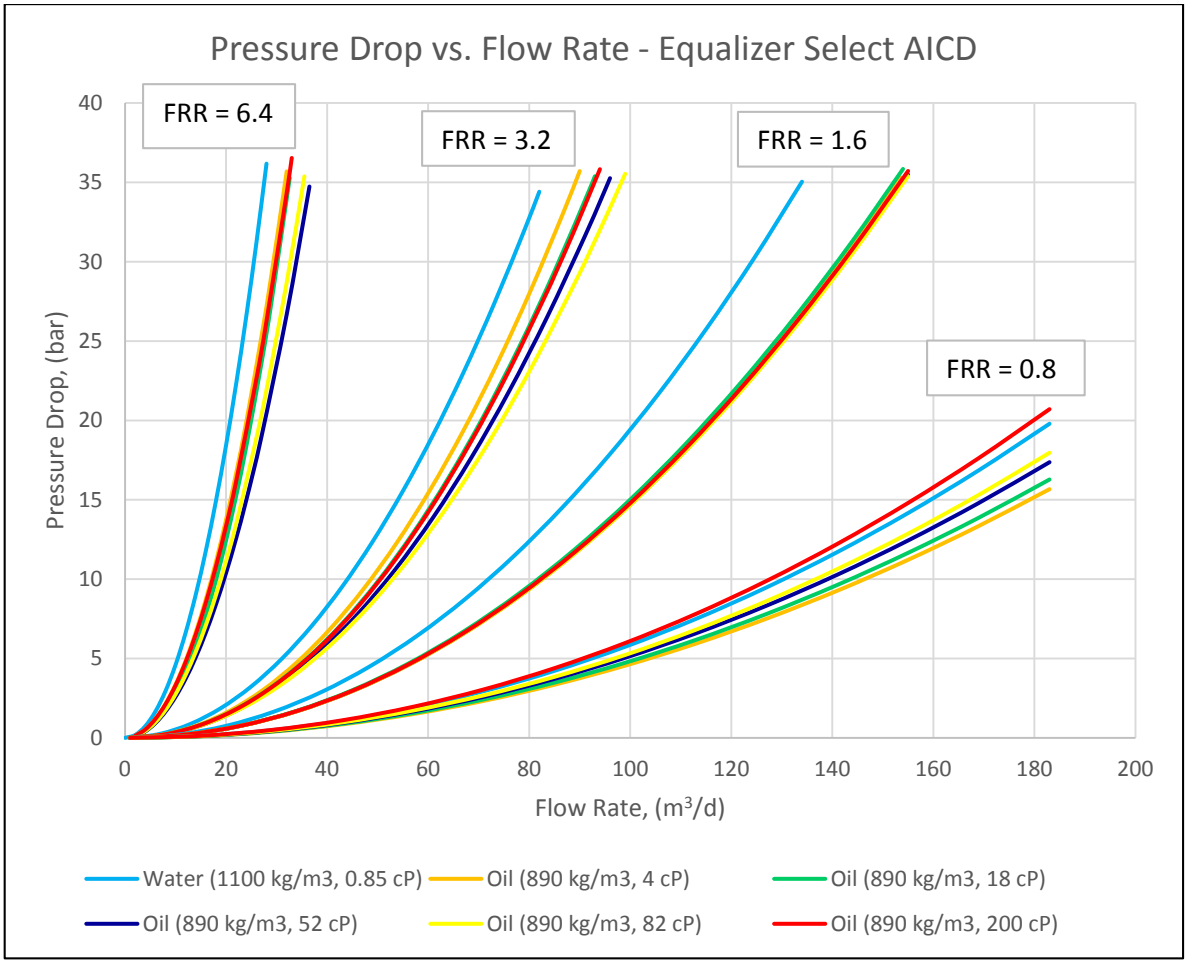

Figure 33: Performance curves for Equalizer Select AICD, pressure drop dependence of flow rate, (Akbari, 2014)

Figure 33 shows the flow performance of each of the FRR settings of the device starting from highest 6.4, to lowest 0.8, respectively. It can be seen that the fluids with a wide range of viscosities from 0.85 cP to 200 cP are grouped, with small margins, for every FRR setting. Based on that, it can be concluded that pressure drop is dependent on the FRR setting of the device, and therefore dependent on the pressure loss coefficient (K), which is different for every FRR setting.

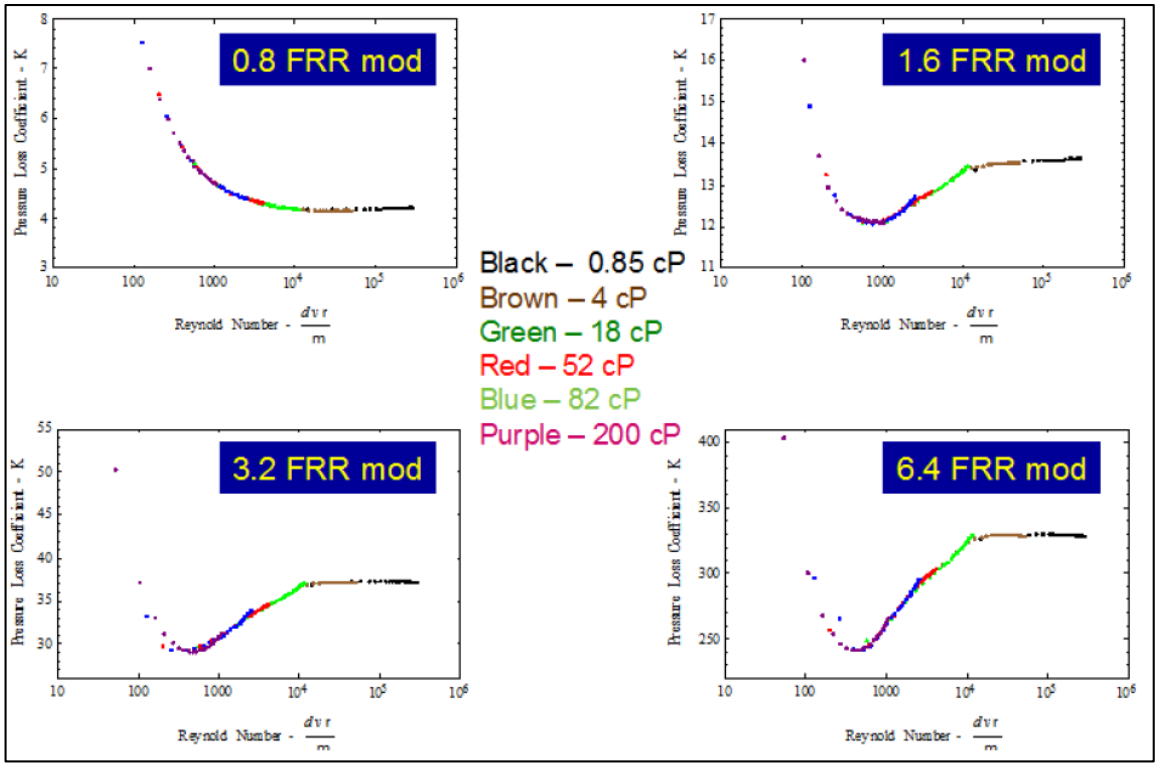

Figure 34: Pressure loss coefficient (K) dependence on FRR setting of Equalizer Select AICD and Reynolds Number, (Akbari, 2014)

Figure 34 shows the pressure loss coefficient change with the change in Reynolds number, for the different FRR settings. As the pressure loss coefficient increases, pressure drop also increases. For lowest FRR setting of 0.8, pressure drop is higher for Reynolds number up to 1000, which is in the laminar flow regime. Therefore, the pressure drop will be the largest for high viscosity fluids (oils), and it will go down for lower viscosity fluids (water and gas), respectively. For other FRR settings, 1.6, 3.2 and 6.4, one trend line is established. Here, there is a drop in pressure drop for higher viscosity fluids as the Reynolds number reaches the values around 1000 – 2000, which is the limit for the laminar flow regime. As the Reynolds number increases over that limit, and goes to transitional and turbulent flow regime, respectively, pressure drop increases for lower viscosity fluids. Going from a FRR setting of 1.6 up to FRR setting 6.4, pressure drop increases respectively, with the increase in the Reynolds number, with following the similar trend line.

Performance data calculated from experimental data and Figure 33, using the method described in the Methodology chapter of this thesis, are presented in table 4.

Table 4: Performance data (C, c), for Equalizer Select AICD

	(C, n)	*FRR= 0.8*	*FRR=1.6*	*FRR=3.2*	*FRR=6.4*
Water (1100 kg/m^3, 0.85 cP)	**C**	0.00055	0.0018	0.0054	0.0459
	n	***2.0138***	***2.0165***	***1.9878***	***2.0016***
Oil (890 kg/m^3, 4 cP)	**C**	0.00044	0.0014	0.0032	0.0315
	n	***2.0118***	***2.0132***	***2.0712***	***2.0292***
Oil (890 kg/m^3, 18 cP)	**C**	0.00046	0.0014	0.0031	0.021
	n	***2.0106***	***2.0152***	***2.0612***	***2.1314***
Oil (890 kg/m^3, 52 cP)	**C**	0.00049	0.0014	0.0031	0.0256
	n	***2.0109***	***2.0106***	***2.0533***	***2.0051***
Oil (890 kg/m^3, 82 cP)	**C**	0.00051	0.0014	0.0032	0.0266
	n	***2.0097***	***2.0101***	***2.0272***	***2.0151***
Oil (890 kg/m^3, 200 cP)	**C**	0.00055	0.0014	0.0031	0.0325
	n	***2.0225***	***2.0119***	***2.0591***	***2.0091***

By analyzing data from table 4, it is calculated that the flow rate exponent of the Equalizer Select AICD is around 2.03 (n=2.03). Flow rate exponent remains fairly constant, the change in the curves is shaped by the proportionality constant (C), which is different for different FRR setting. From there it can be concluded, that the proportionality constant (C) for this device is mostly controlled by a pressure loss coefficient (K), and therefore with the fluid properties (viscosity and density). And with the increase in the choking effect, for the different settings of the FRR, proportionality constant (C) is increasing.

4.4.1.1 Equalizer Select vs. ICD – nozzle Performance Comparison

Both devices will be tested with the flow of water and oil. In addition, for Equalizer Select all its FRR settings will be included, in order to see the difference between the devices.

Fluids used for performance comparison:

- Water: density 1100 kg/m^3, viscosity 0.85 cP;
- Oil: density 890 kg/m^3, viscosity 18 cP.

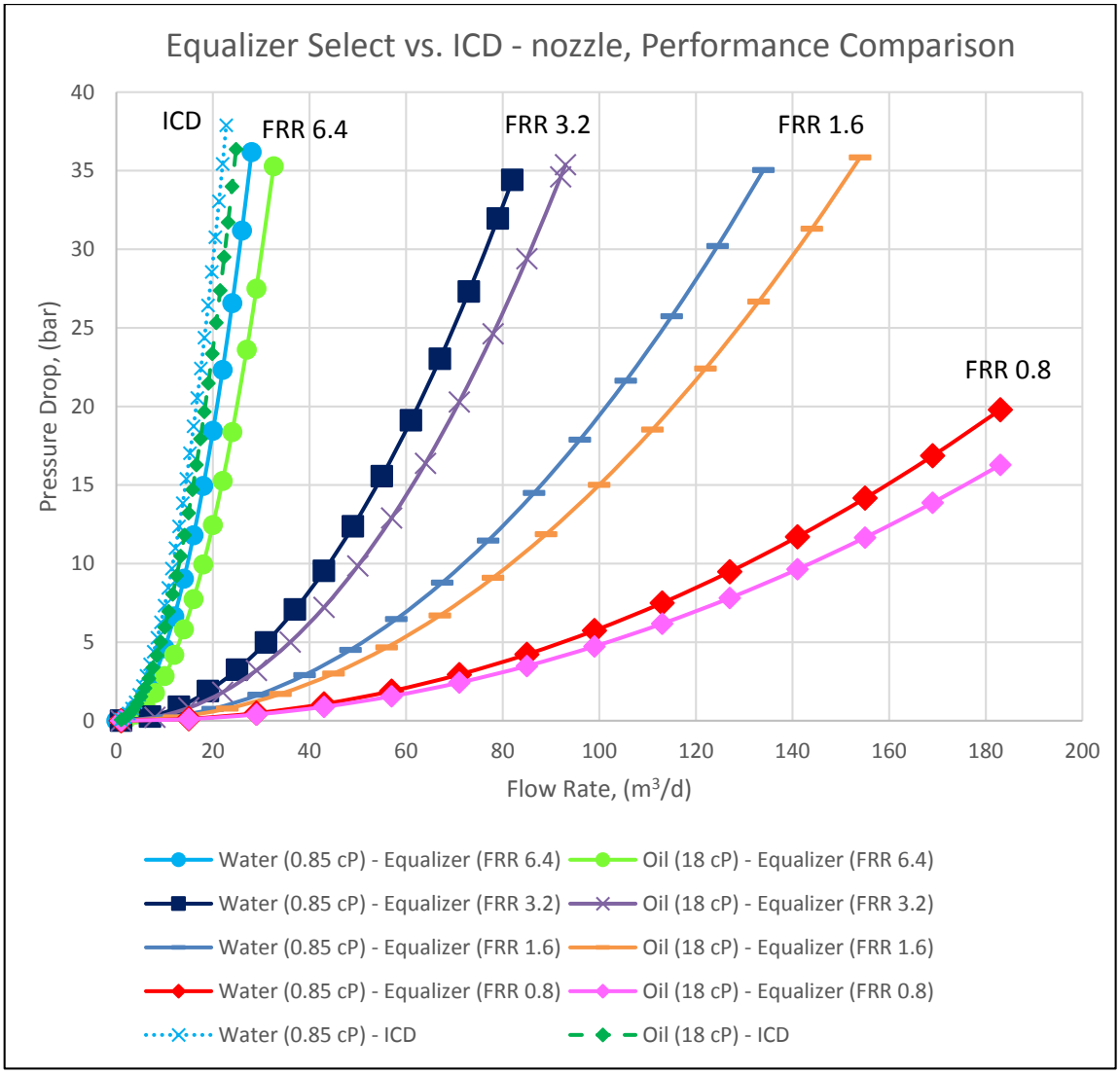

Figure 35: Comparison between Equalizer Select and ICD - nozzle performance characteristics

Figure 35 shows that the choking effect between ICD- nozzle and highest FRR (6.4) settings for Equalizer Select AICD, are the same. Comparing other FRR settings with the ICD – nozzle, shows the advantage of the Equalizer Select AICD. Its main strength compared to the ICD – nozzle, is its adjustability. Equalizer Select is able to choke the production same as the ICD – nozzle, where it is necessary. On the other hand, it can also provide lower choking effect in zones where there are no problems with unwanted fluids breakthrough. All of these FRR settings, are packed into one device. For the Equalizer Select to be applied correctly, detailed information about the reservoir properties are necessary, especially the permeability distribution through the producing reservoir section.

4.5 Wormhole AICD Principles

As it is covered in the chapter 2 of this thesis, principles that are used in developing Wormhole AICD are based on keeping the flow rate within the preset range of the device setup by adjusting the hydraulic impedance of the device. The device is comprised of input and output openings. In between, there is at least one sequential stage of the labyrinth pressure drop pathway, similar to the Equalizer Select AICD, and one flow dependent autonomous shut off valve (Figure 36).

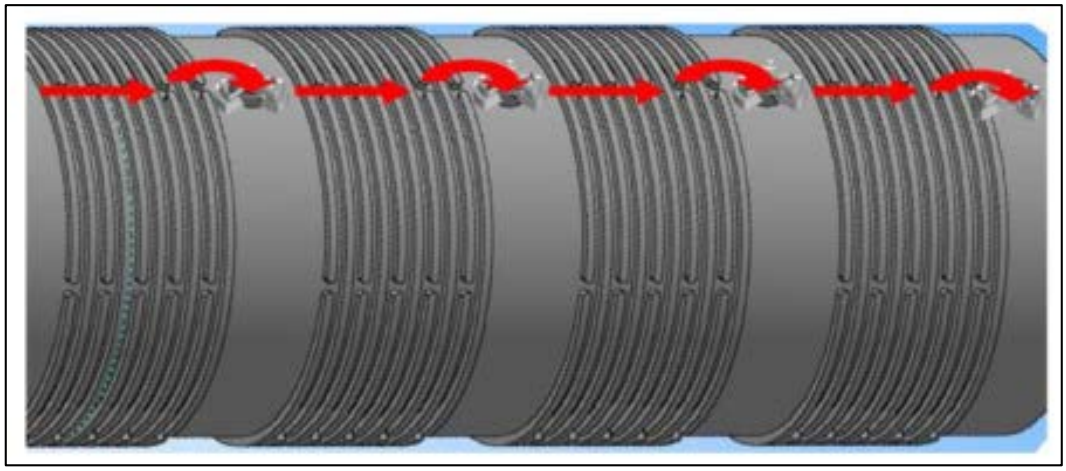

Figure 36: Wormhole AICD, with four labyrinth type pressure drop pathways, and four shut off valves, (Delia et al., 2015)

The operation of the shut off valves used in the Wormhole AICD is based on two physical phenomena, magnetism and hydrodynamics. For the valve to stay open, the pressure due to impact velocity and hydraulic impedance of the flowing fluid, together with pressure reduction in high flow rate areas, change the pressure on the gate side of the valve. The magnetic force that is keeping the gate (ball) in the open position counteracts the pressure at the gate side. As long as, the magnetic force is greater than the pressure on the gate side, the valve is in the open position. When the pressure at gate side overcomes the magnetic force that is holding the gate, the valve is pushed towards the valve saddle (1) and the valve closes (Figure 37). (Volkov et al., 2014).

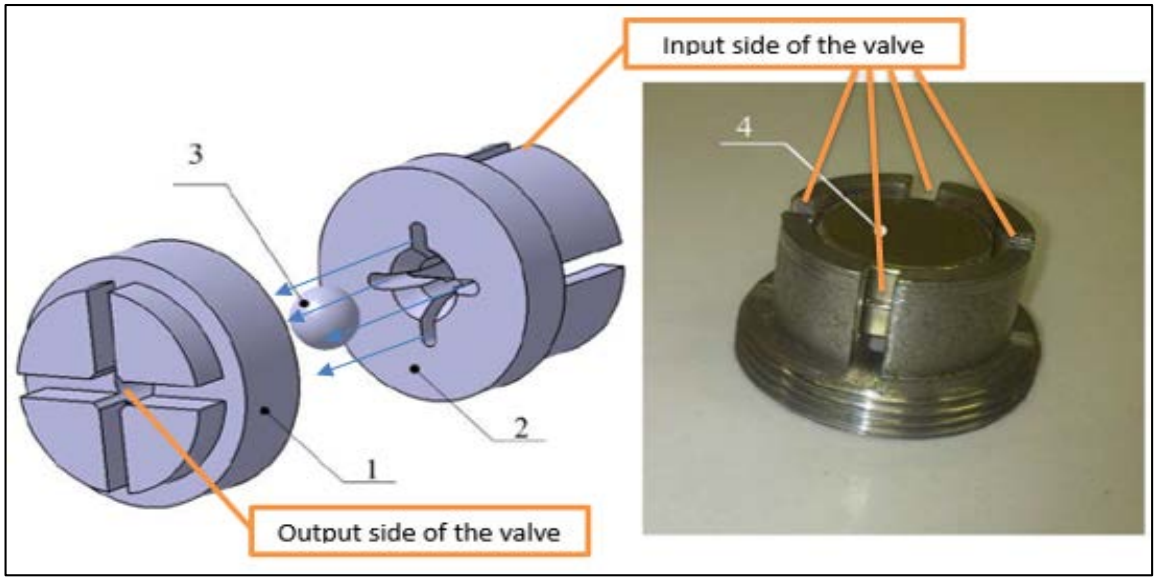

Figure 37: Shut off valve design, on the left three-dimensional model of the valve; on the right valve gate retaining component; (1 – valve saddle; 2 – valve cap; 3 – gate; 4 – magnets), (Volkov et al., 2014)

If the flow rate is still over the preset value after the firs valve closes, the rest of the valves will keep closing one by one in line, respectively. When the flow rate of the fluid through the AICD is less than nominal, the force of permanent magnets will pull the gates back in the open position, and allow the circulation through the valves.

Wormhole AICD has a similar function as the AFD valve presented in this chapter. Its main objective is keeping the flow rate at predetermined ranges, by regulating the hydraulic impedance of the flowing fluid.

4.5.1 Wormhole AICD Performance

By analyzing experimental data from (Delia et al., 2015), Wormhole AICD performances have been tested on the flow of liquids (water) and gas (air), in order to see the effect of Wormhole AICD design.

Fluids used for performance testing:

- Water: density 1100 kg/m^3, viscosity 1 cP;
- Gas (air): density 120 kg/m^3, viscosity 0.017 cP (at 15˚C).

Liquid flow rate testing:

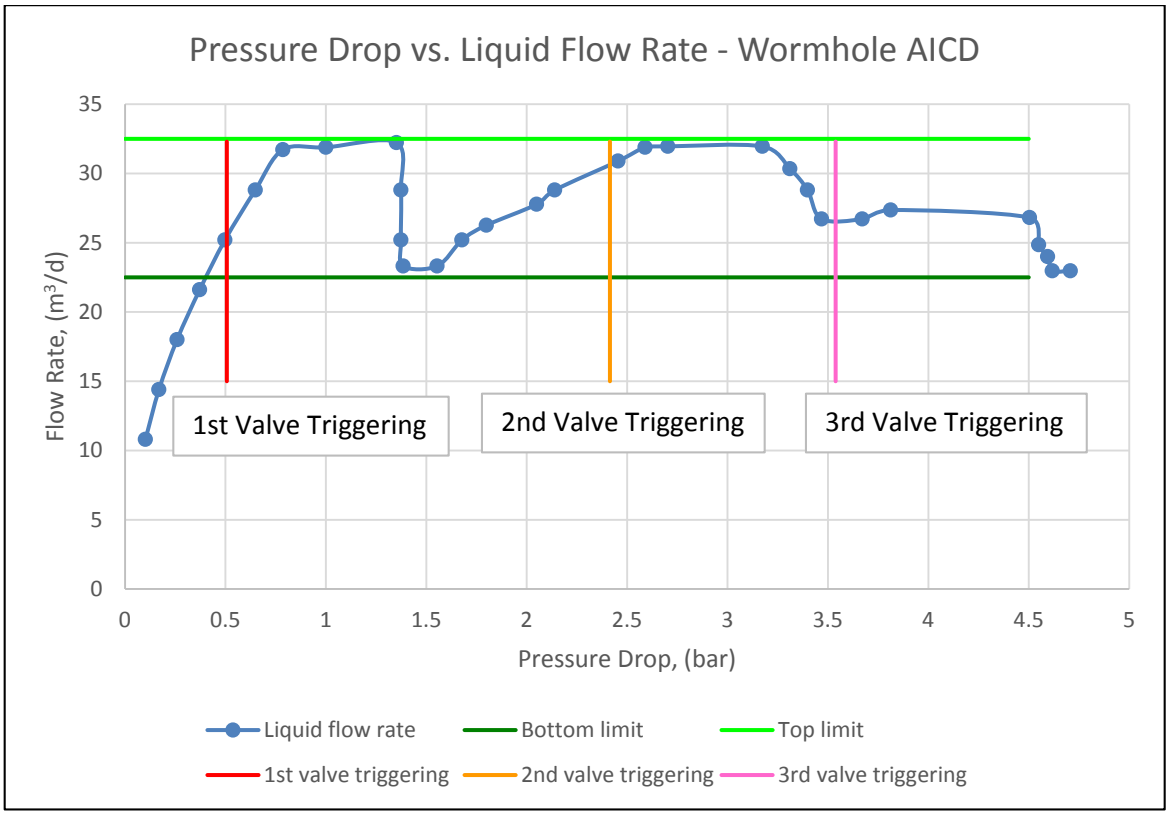

Figure 38: Performance curve for liquid (water) flow through Wormhole AICD, pressure drop dependence of flow rate, (Delia et al., 2015)

Figure 38 shows the performance of liquid flow rate through Wormhole AICD. Since it is flow rate controller device, it can be seen that flow rate is increasing towards the preset limit of the valve opening. When the pressure due to the velocity impact, reaches the limit of first valve, it closes and the decreases the flow rate with the increase in the pressure drop. Flow continues towards the second and third valve and they are closing in the same pattern, keeping the flow rate in the preset limits. In these settings, it can be seen that the flow rate limits are between 22.5 m^3/d up to 32.5 m^3/d.

Gas (air) flow rate testing:

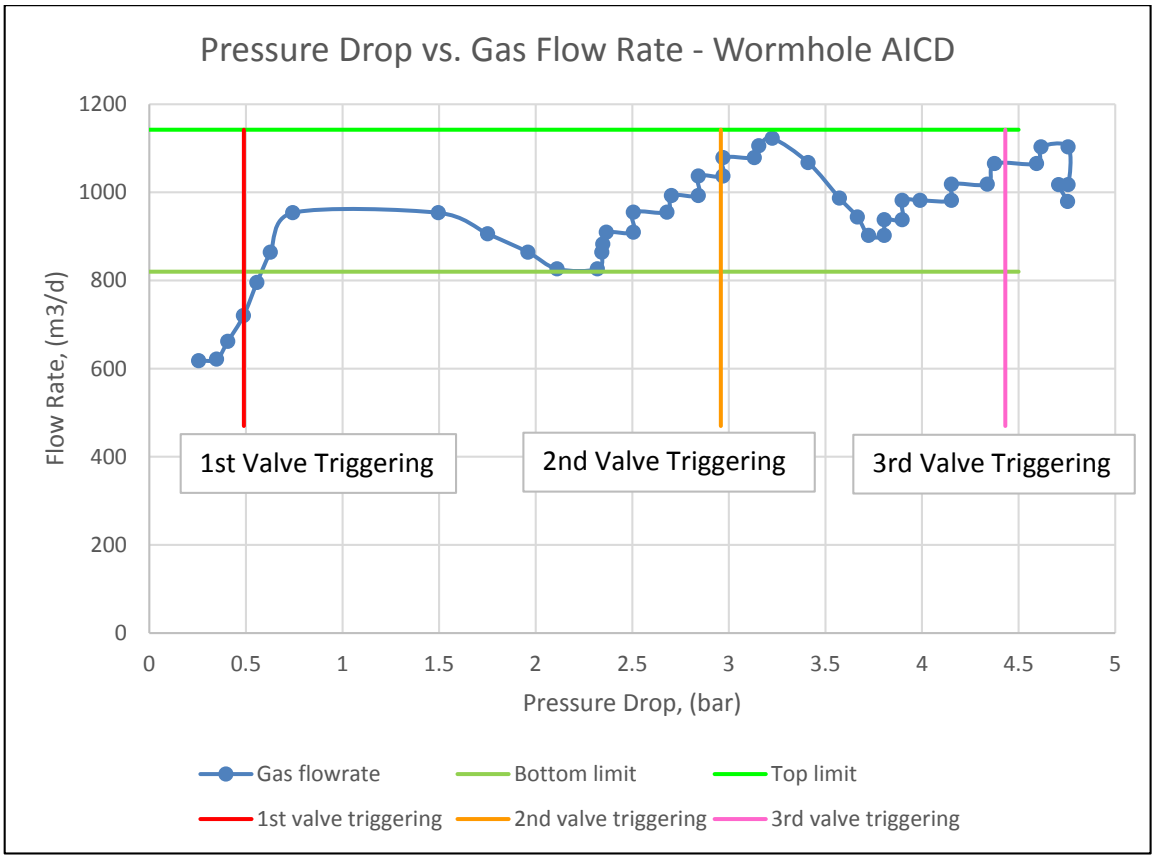

Figure 39: Performance curve for gas (air) flow through Wormhole AICD, pressure drop dependence of flow rate, (Delia et al., 2015)

Figure 39 shows the performance curve for the flow of gas (air) through the Wormhole AICD. By looking at Figure (38), it can be observed that the behavior of the device is very similar compared with the liquid flow. The values of the flow rate of gas are much higher for the same pressure drop, compared to the liquid flow through the device. Valves are triggering one by one from first to third, respectively. The flow rate preset limits for gas flow and these settings are 820 m^3/d up to 1142 m^3/d, respectively.

The performance data are not going to be calculated for the Wormhole AICD, because it is not possible to cover these type of performances with the method described in the Methodology chapter of this thesis.

4.6 Floating - Flapper Valve Principles

The Floating – Flapper Valve is based and designed on the Archimedes' principle. The Archimedes' Principle states that submerged solid will be subjected to the buoyancy force equal in magnitude to the weight of the fluid it displaces. The buoyancy force acts on the solid's center of gravity. If the solid is heavier the buoyancy force acting on it, it will sink. If it is lighter than the buoyancy force, it will float.

The design of the Floating – Flapper valve uses this principle in the form of the counterweight floating flapper (Figure 40).

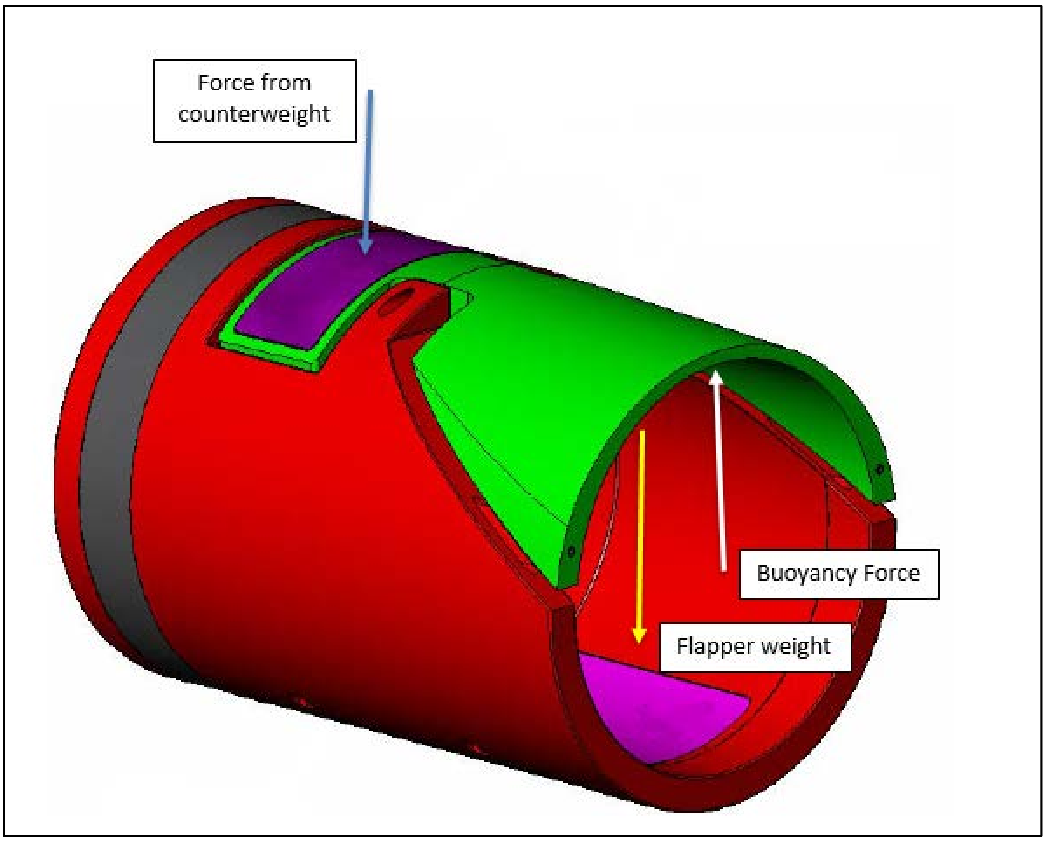

Figure 40: Floating - Flapper valve working principle, force balance, (Crow et al., 2006)

The mass of the counterweight is the regulating parameter for changing the settings of the floating – flapper valve depending on the properties of the fluid.

Buoyancy force can be represented through the Buoyancy factor (BF) (equation 10).

$$\mathrm{BF} = 1 - \frac{\rho_{fluid}}{\rho_{material}} \dots\dots\dots\dots\dots\dots\dots\dots\dots\dots\dots\dots\dots\dots. (10)$$

Where: BF – Buoyancy Factor;

ρ_{fluid} – density of the flowing fluid;

$\rho_{material}$ – density of the flapper material.

To keep the valve in open position, the force on the counterweight side of the valve has to be greater than the force on the flapper side, acting downwards, due to the mass of the flapper itself. Since the area of the counterweight is significantly smaller, compared to the floating flapper, the buoyancy force acting on that side can be neglected. In that case, force balance will look like in the equation 11.

$$F_{counterweight} > F_{flapper} * BF \dots\dots\dots\dots\dots\dots\dots\dots\dots\dots\dots (11)$$

Where: $F_{counterweight}$ – Force from the counterweight;

$F_{flapper}$ – force from the flapper weight;

BF – buoyancy factor.

Taking steel to be the material of which the flapper is made, density of steel is around 7800 kg/m^3, which would represent the flapper material density ($\rho_{material}$). Including density of the flowing fluid to be in the range from 120 kg/m^3 for gas flow, and 1100 kg/m^3 for water flow, respectively. Using the equation 10 for BF, BF will vary in the range from 0.859, for gas density, to 0.985 for water density, as two extremities.

Considering those two values for BF, and combining it with the equation 11, it is observed that for higher BF, force flapper weight ($F_{flapper}$) has greater value, and in this case, the valve is in closed position, and the force balance is presented in the equation 12.

$$F_{counterweight} < F_{flapper} * BF \dots\dots\dots\dots\dots\dots\dots\dots\dots\dots\dots (12)$$

How the value for BF decreases, as the fluid density increases, the force balance will look like it is explained in equation 11 above. Therefore, the Floating – Flapper valve will be in open position. As the density of the fluid decreases, the buoyancy force will decrease, and the valve will start closing.

Performance characteristics of the Floating – Flapper valve are controlled by the ICD – nozzle, installed in the completion string, as it is mentioned in the chapter 2 of this thesis. Principles of ICD – nozzle are explained at the beginning of this chapter. Floating – Flapper valve, since it is density controlled, is primarily designed to be a gas stopper valve.

4.6.1 Floating – Flapper Valve Performance

Considering the principles elaborated above, performance characteristics of the Floating – Flapper valve are the same as for ICD – nozzle, for liquid phases. But for the gas flow, choking effect is expected to be higher compared to the ICD – nozzle. The device will start closing after some time, when the gas start flowing.

Fluids used for performance testing:

- Water: density 1100 kg/m3, viscosity 1 cP;
- Oil: density 849 kg/m3, viscosity 10 cP;
- Gas: density 103 kg/m3, viscosity 0.02 cP.

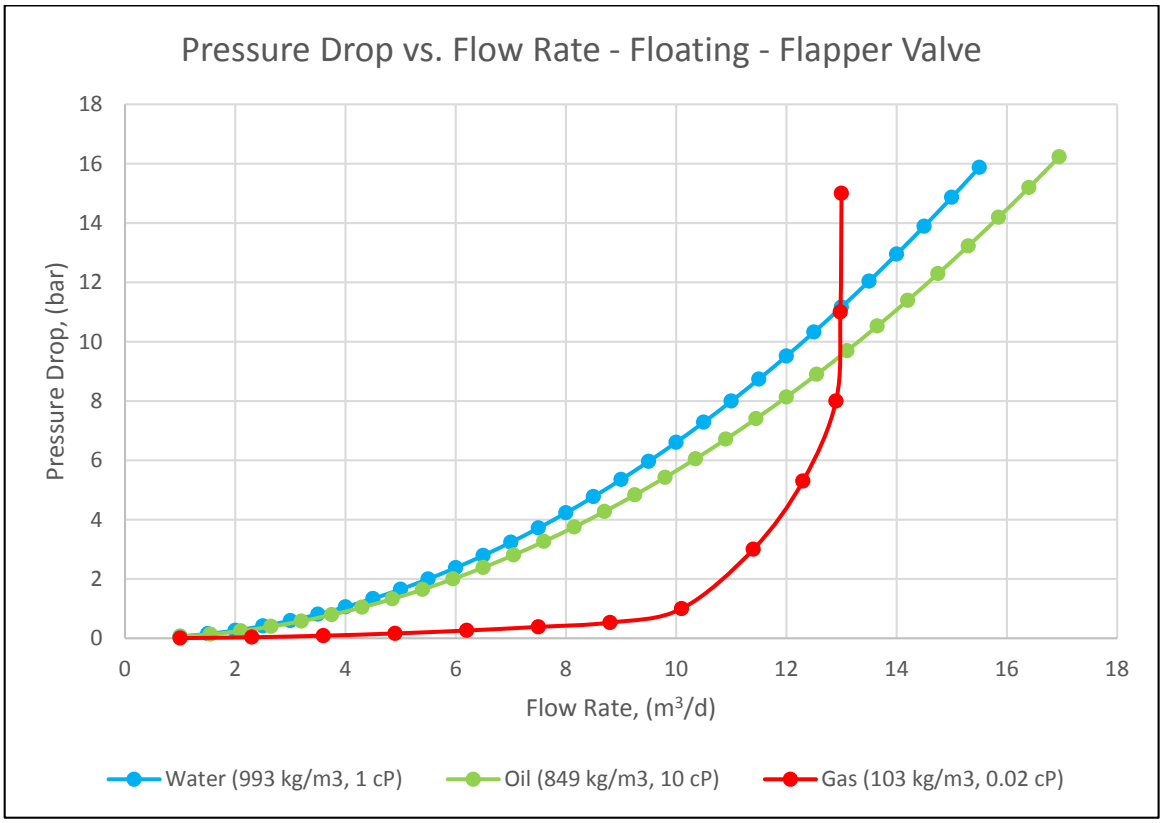

Figure 41: Performance curves for Floating - Flapper Valve, pressure drop dependence of flow rate

Analyzing Figure 41, it can be seen that flow performance for water and oil are unchanged compared to the ICD – nozzle. As for the gas flow, Figure 41 shows a buffer period, when the gas starts flowing, until the device closes completely. Since the lack of experimental data, this buffer period is assumed, due to the well flowing conditions. After the buffer period, the gas production is completely stopped, due to the reduction in the buoyancy forces, which keep the device open.

The performance data for Floating – Flapper valve are the same as for ICD – nozzle, the flow rate exponent is equal to 2 (n=2).

Since there are no differences between Floating – Flapper Valve and ICD – nozzle for the liquid flow (water and oil), the comparison is not necessary. One important thing to mention, is the flow of gas phase, which is stopped after a short period of time with the Floating – Flapper valve, compared to the ICD – nozzle.

4.7 RCP valve Principles

The RCP valve is based on the Bernoulli's principle as described by (Halvorsen et al., 2012; Mathiesen et al., 2011). By neglecting, the elevation and compressible effects, the Bernoulli's equation can be expressed as shown in the equation (13) (Figure 42):

$$P_1 + \frac{1}{2}\rho v_1^2 + \Delta P_{friction\ loss} = P_2 + \frac{1}{2}\rho v_2^2 \ldots\ldots\ldots\ldots\ldots\ldots\ldots\ldots\ldots (13)$$

Where: P_1 – reservoir pressure (static);

P_2 – stagnation pressure (static);

$\frac{1}{2}\rho v^2$ – dynamic pressure;

$\Delta P_{\text{friction loss}}$ – frictional pressure loss along the streamline.

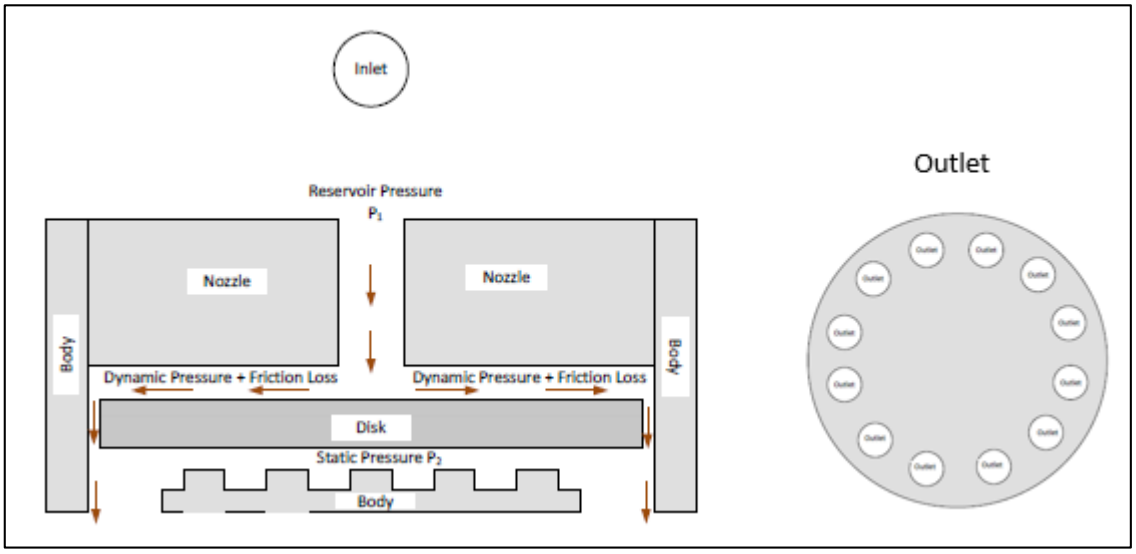

Figure 42: Cross sectional schematic view of RCP valve, with pressure distribution through the device, (Isma Mohd, 2014)

As described in the chapter 2 of this thesis, the RCP valve is designed in that way that it chokes the flow of low viscosity fluids, as part of its flow control ability. When gas starts flowing through the valve, as the fluid with lowest viscosity, the disc will move towards

the seats, and restricts the flow area. The pressure will be lower at the flowing side of the disc (Bernoulli Effect) due to large gas velocity (dynamic pressure). Since the streamlines of the gas flow, as a low viscous fluid will follow the inner flow area of the valve, close to the limits of the valve itself, the pressure behind the disc will be higher. The higher the pressure behind the levitating disc, more the disc will be moved towards the seats of the valve, due to the pressure difference between two sides. Compared to the gas flow, the oil as a fluid with higher viscosity, will tend to follow the different streamlines through the valve. Viscous forces will keep the fluid follow more smooth streamlines through the device. Hence, the stagnation pressure behind the disc, will be much smaller compared to the gas flow. Therefore, the pressure difference will be smaller, and the disc will be in the fully open position (Figure 42) (Halvorsen et al., 2012; Mathiesen et al., 2011).

The RCP valve is firstly developed to be a gas isolation valve, but it can also be applied as a water stopper in a heavy oil reservoirs, with higher viscosity ranges.

4.7.1 RCP valve Performance

Analyzing the experimental data presented in the following papers (Halvorsen et al., 2012; Halvorsen et al., 2016; Mathiesen et al., 2011; Voll et al., 2014), performance results are developed.

Fluids used for performance testing:

- Gas: density 150 kg/m^3, viscosity 0.02 cP;
- Water: density 1100 kg/m^3, viscosity 0.45 cP;
- Oil: density 890 kg/m^3, viscosity 2.7 cP;
- Oil: density 890 kg/m^3, viscosity 10 cP;
- Oil: density 890 kg/m^3, viscosity 35 cP;
- Oil; density 890 kg/m^3, viscosity 90 cP.

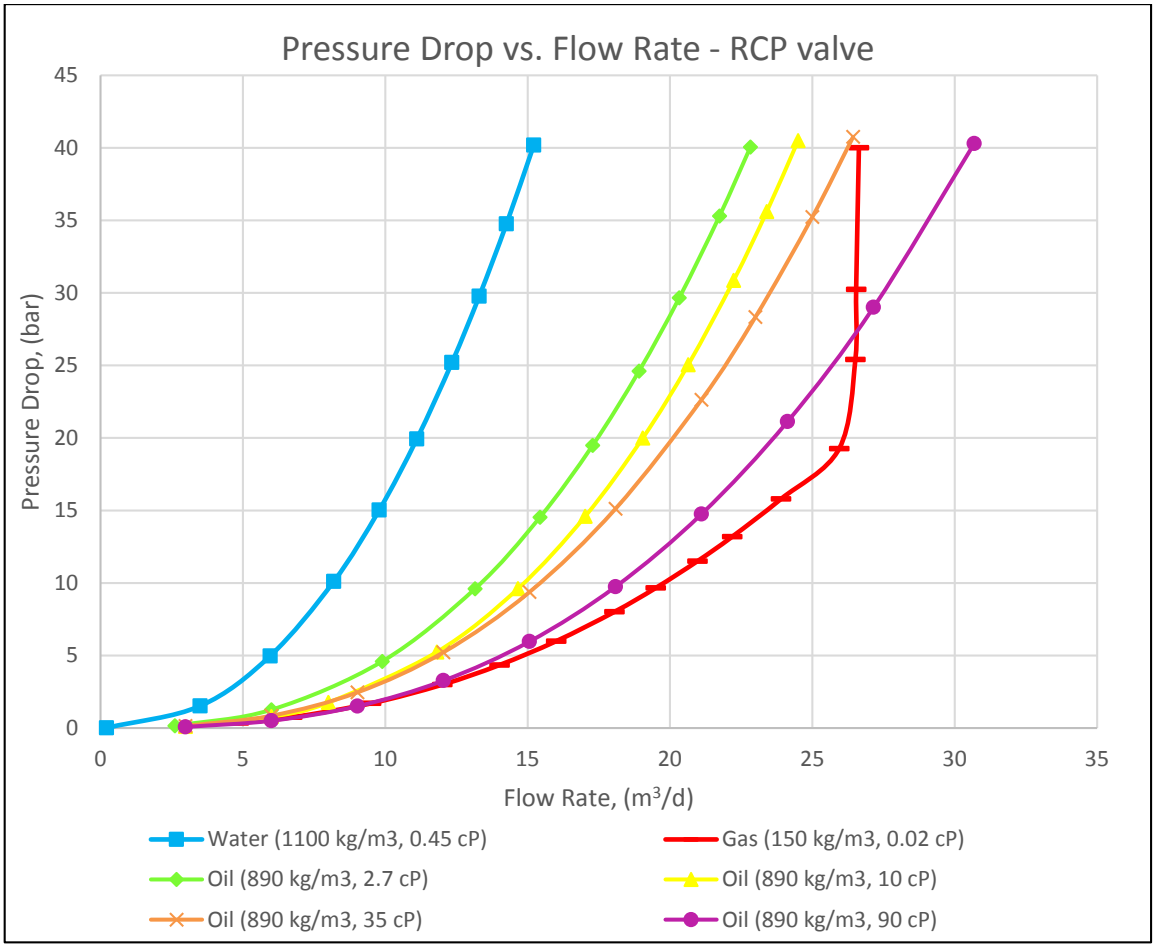

Figure 43: Performance curves for RCP – valve, pressure drop dependence of flow rate

Figure 43 shows the flow of water, gas and different types of oils. Firstly, it can be seen that choking of gas flow follows the trend line up to the critical flowrate. In this case, the critical flow rate is around 26 m^3/d, for this gas properties. At that point, floating disc in the valve will almost completely restrict the flow of gas. The pressure difference at this point is high, due to the Bernoulli Effect, and high entry velocity of the gas and low viscosity of it. This is the primary function of the RCP valve, as it was firstly developed as a gas stopper valve for the Troll field in the Norwegian Continental Shelf (NCS).

Secondly, comparing the flow of water and oils, it is obvious that choking effect is higher for water than it is for any of the oils. Since the RCP valve is viscosity dependent, therefore the flow through it changes due to the change of fluid viscosity. Therefore, usage of RCP valve in light oil reservoirs with water presence, is not recommended, because the small margin between viscosities. Oppositely, in reservoirs with a combination of heavier oils and water, with a wide range of viscosity difference, it can be used.

Calculated data, which is developed, and it is used for describing the performance of the RCP valve, is presented in table 5 bellow.

Table 5: Performance data (C, n), for RCP valve

	Proportionality Constant (C)	Flow Rate Exponent (n)
Gas (150 kg/m^3, 0.02 cP)	0.0073	2.4195
Water (1100 kg/m^3, 0.45 cP)	0.0928	2.2302
Oil (890 kg/m^3, 2.7 cP)	0.0121	2.5912
Oil (890 kg/m^3, 10 cP)	0.0052	2.8013
Oil (890 kg/m^3, 35 cP)	0.0078	2.6145
Oil (890 kg/m^3, 90 cP)	0.0041	2.6851

Analyzing the results from Table 5, it can be seen that average flow rate exponent (n) for RCP valve is around 2.6 (n=2. 6). Which indicates the high impact of the change in the flow area and the velocity of the flowing fluid. As for the proportionality constant (C), with the decrease in the viscosity of the fluid, (C) is increasing, together with the choking effect.

4.7.1.1 RCP valve vs. ICD Performance Comparison

In this subchapter, flow performance of RCP valve and ICD nozzle is going to be compared. In order to see the differences between RCP valve and ICD – nozzle, devices are tested on flow of gas, water and oil with the same properties.

Fluids used in performance testing:

- Gas: density 150 kg/m^3, viscosity 0.02 cP;
- Water: density 1100 kg/m^3, viscosity 0.45 cP;
- Oil: density 890 kg/m^3, viscosity 10 cP.

The performance curves are presented in Figure 44 bellow.

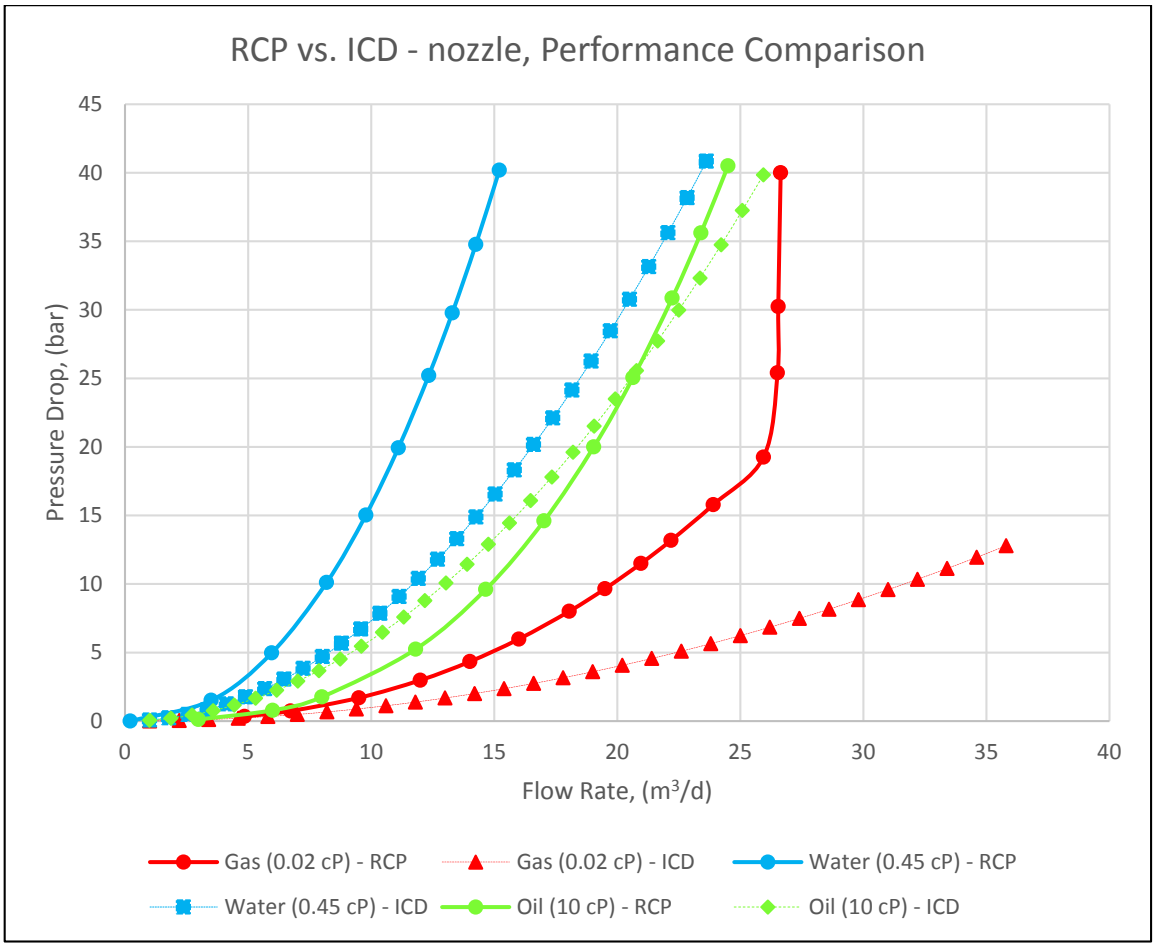

Figure 44: Comparison between RCP valve and ICD - nozzle performance characteristics

Figure 44 shows the differences between RCP valve and ICD – nozzle. Starting from water flow, it can be seen that pressure drop progression (choking effect) is higher for RCP valve than it is for an ICD. Comparing that with the flow of oil, it is noticeable that the choking is very similar, in order to prevent an early breakthrough of unwanted fluids. On the flow of oil, the difference in flow rate exponent can be seen more easily. For ICD – nozzle is 2 (n=2) and for RCP – valve is around 2.6 (n=2.6).

As for the gas flow, the pressure drop progression is higher for RCP – valve compared to the ICD – nozzle. In addition to that, it can be observed, that after critical flow rate, when the RCP disk closes, pressure drop dramatically increases. Where with the ICD it follows the previous trend line.

4.8 AICV Principles

The principles that used to develop AICV technology is based on the Poiseuille's law for laminar restrictor and Bernoulli's principle for the turbulent flow restrictor. Both laminar and turbulent restrictors are place in series, respectively (Mathiesen et al., 2014).

Laminar flow restrictor can be considered as pipe segment and the pressure drop can be expressed as (equation 14) (Aakre et al., 2014):

$$\Delta P = f * \frac{L * \rho * v^2}{2 * D} = \frac{64}{Re} * \frac{L * \rho * v^2}{2 * D} = \frac{32 * \mu * v * L}{D^2} \; \alpha \; \mu v \; \ldots\ldots (14)$$

Where: ΔP – pressure drop;

f – friction factor (64/Re);

ρ – fluid density;

μ - fluid viscosity;

v – fluid velocity;

L, D – length and diameter of the laminar flow restrictor respectively.

The pressure drop through the laminar flow restrictor is proportional to the fluid viscosity and velocity.

Turbulent flow restrictor follow the behavior of a thin plate orifice and the pressure drop can be expressed as (equation 15) (Aakre et al., 2014):

$$\Delta P = k * \frac{1}{2} * \rho * v^2 \; \alpha \; \rho v^2 \; \ldots\ldots\ldots\ldots\ldots\ldots\ldots\ldots\ldots\ldots\ldots\ldots\ldots\ldots (15)$$

Where: k – geometrical constant;

The pressure drop through the turbulent is proportional to the fluid velocity and fluid velocity squared.

Figure 45 and 46 respectively, show the pressure drop versus the velocity through the laminar and turbulent flow restrictors for heavy oil, water and gas.

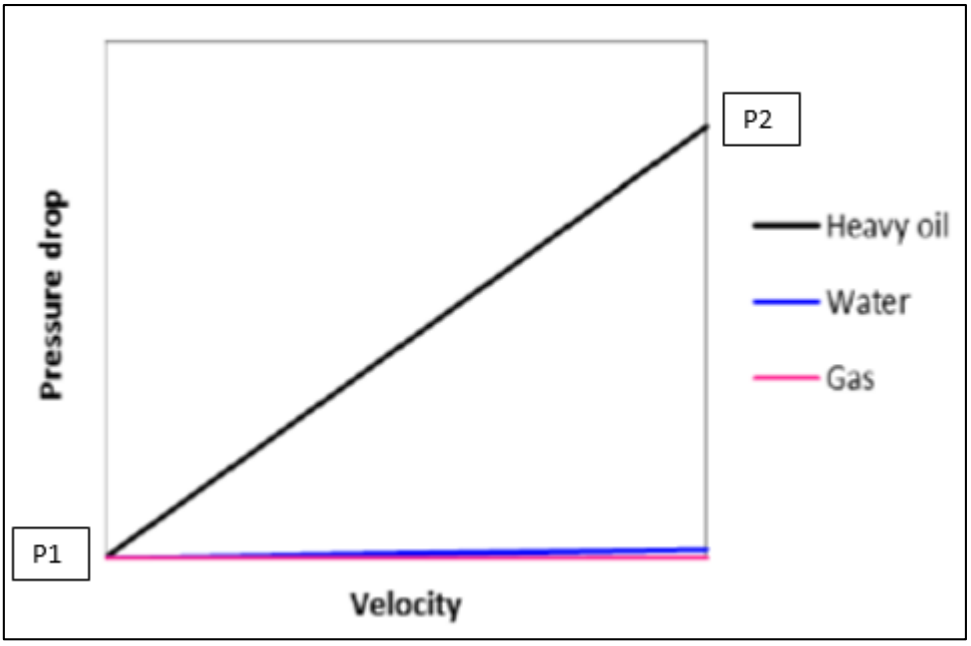

Figure 45: Pressure Drop vs. Velocity through the laminar flow restrictor, (Aakre et al., 2013)

From figure 45, it can be seen that the heavy oil, with a much higher viscosity compared to the water and gas, experiences high pressure drop with the increase of velocity. On the other hand, water and gas as low viscous fluids do not suffer almost any pressure drop, when flowing through laminar restrictor. This is explained by the equation 14, where for the laminar restrictor, pressure drop is governed mainly by the fluid viscosity and velocity. Pressure at the entrance in laminar restrictor is the inlet pressure (P1), which is reduced to the pressure (P2) after the laminar restrictor.

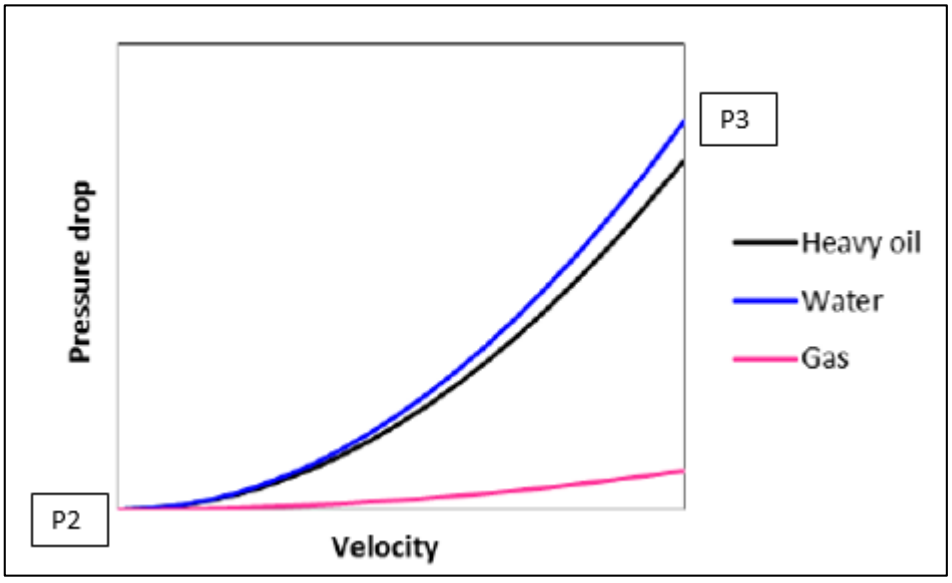

Figure 46: Pressure Drop vs. Velocity through the turbulent restrictor, (Aakre et al., 2013)

Figure 46 shows, the pressure drop in the turbulent restrictor with the increase in the

velocity of the flowing fluids. Heavy oil and water experience higher pressure drop, since the turbulent restrictor is controlled with the density and squared velocity of the flowing fluid, due to higher density, as showed in the equation (15). Gas experiences a pressure drop mainly because of the squared velocity term. But the entry pressure, before turbulent restrictor (P2), for heavy oil is smaller compared to the water and gas, since the pressure drop is much higher for oil in the laminar restrictor before. Pressure after fluids exit the turbulent restrictor is marked with (P3).

Therefore, based on the information above, the pressure (P2), in between the laminar and turbulent restrictor, will change if the properties of the fluid change (viscosity or density).

As described in the chapter 2 of this thesis, the choking element in the device is the floating disc inside the body of the valve. It is controlled by the force difference between top and bottom side. Top side of the disc, has a smaller area (A1) compared to the bottom side area (A2). The inlet pressure in the device (P1), is acting on the top side of the disc area (A1), producing the force (F1), which acts downwards and pushes the AICV in “open” position. The pressure (P2), after the fluid passes through the laminar restrictor, acts on the bottom, larger area of the disc (A2), producing the force (F2), which acts upwards pushing the valve in “close” position. The difference between these two forces (F1-F2) will determine whether the AICV is going to be in an opened or closed position. If the force difference is positive, the valve will be in opened position, if it is negative, it will be in closed position (Figure 47). Since the inlet pressure (P1) is always higher than the pressure (P2), therefore the area (A2) has to be larger than the area (A1). The ratio between surfaces (A1) and (A2) is a design parameter for the AICV (Mathiesen et al., 2011).

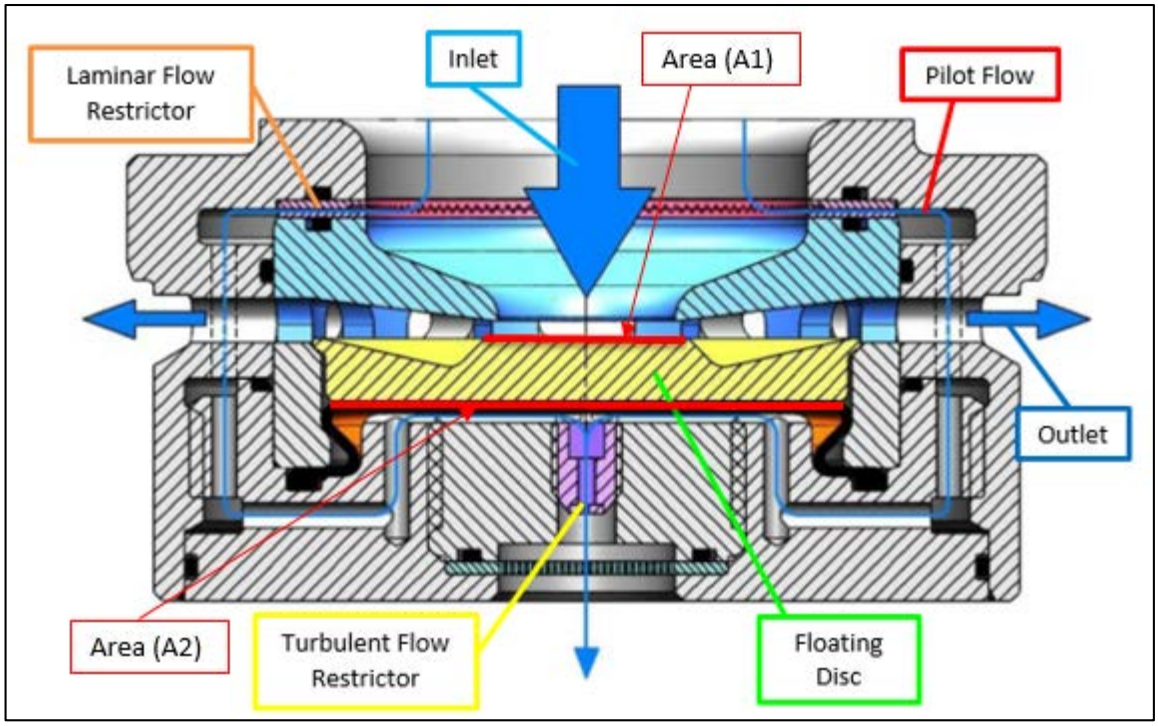

Figure 47: AICV schematic view, showing main operational parts of the device, (Mathiesen et al., 2014)

When the AICV is in closed position, the fluid will still flow through the pilot flow, until there is a change in flowing properties, and the AICV opens the main flow.

4.8.1 AICV Performance

Analyzing the experimental data from papers (Aakre et al., 2014; Mathiesen et al., 2014), performance curves have been developed, using the flow of gas, water and different types of oils.

Fluids used for performance testing:

- Water: density 1100 kg/m^3, viscosity 0.53 cP;
- Gas: density 90 kg/m^3, viscosity 0.02 cP;
- Oil: density 780 kg/m^3, viscosity 5 cP;
- Oil: density 860 kg/m^3, viscosity 50 cP;
- Oil: density 895 kg/m^3, viscosity 200 cP.

The performance curves are presented in the Figure 48 below.

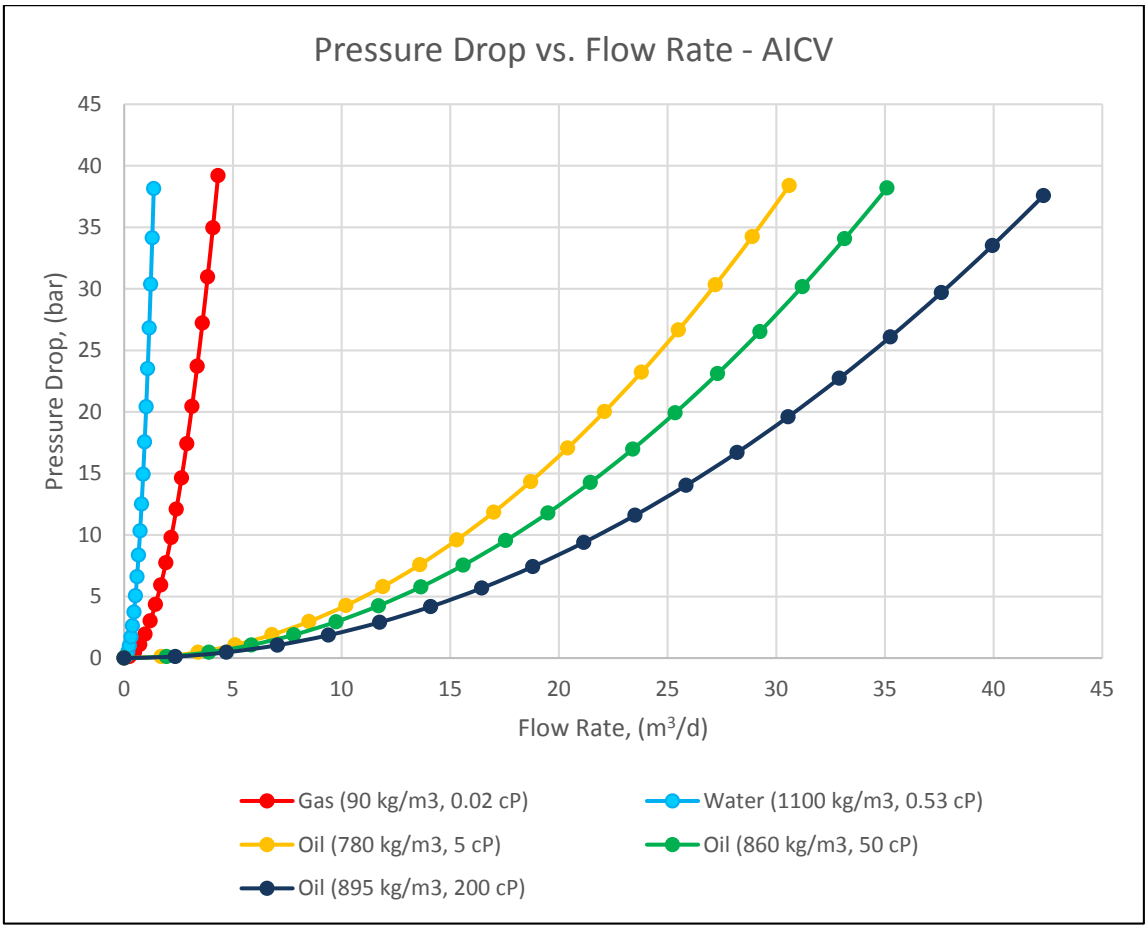

Figure 48: Performance curves for AICV, pressure drop dependence of flow rate

Figure 48 shows, the performance curves for AICV. Examining the curves, it can be noticed the difference between choking intensity for water, gas and oil respectively. Water and gas, as fluids with lower viscosity than oil, experience much higher and almost instantaneous pressure drop. The flow rate for water and gas, which is slightly increased with the increase in pressure drop, is due to the flow through the pilot flow of the AICV.

The reason why the water flow is choked more than the gas flow, is explained by the effect of the turbulent restrictor, and its dependence on density and squared velocity of the fluid. Both water and gas, generate higher pressures in the chamber behind the valve disc (P2), but water as a fluid with higher density is choked more when flowing through the turbulent restrictor, compared to gas flow. Therefore, generating slightly higher pressure beneath the valve disc (P2), compared to gas.

Oil, on the other hand, shows nicely distributed pressure curves, depending on the oil viscosity, primarily. Higher the viscosity, lower is the choking effect, due to the flow

through the laminar restrictor in the device.

Performance data calculated by analyzing experimental data for AICV, is presented in the table 6 below.

Table 6: Performance data (C, n), for AICV

	Proportionality Constant (C)	Flow Rate Exponent (n)
Water (1100 kg/m^3, 0.53 cP)	20	2
Gas (90 kg/m^3, 0.02 cP)	2.1	2
Oil (780 kg/m^3, 5 cP)	0.041	2
Oil (860 kg/m^3, 50 cP)	0.031	2
Oil (895 kg/m^3, 200 cP)	0.021	2

By looking into the data from table 6, it is clear that the average floe rate exponent for the AICV is 2 (n=2). Same as it is for the ICD – nozzle. Evaluating the data for proportionality constant (C), the reason for the higher choking effect of water compared than the gas is clear. Proportionality constant (C) decreases with the decrease in choking effect, and with the increase in fluid viscosity, which is the direct effect of the change in the flowing fluid properties (mainly viscosity).

4.8.1.1 AICV vs. ICD – nozzle Performance Comparison

Both devices have been tested with the flow of one type of water, gas and oil.

Fluids used for performance comparison:

- Water: density 1100 kg/m^3, viscosity 0.53 cP;
- Gas: density 90 kg/m^3, viscosity 0.02 cP;
- Oil: density 780 kg/m^3, viscosity 5 cP.

The performance curves are presented in Figure 49 below.

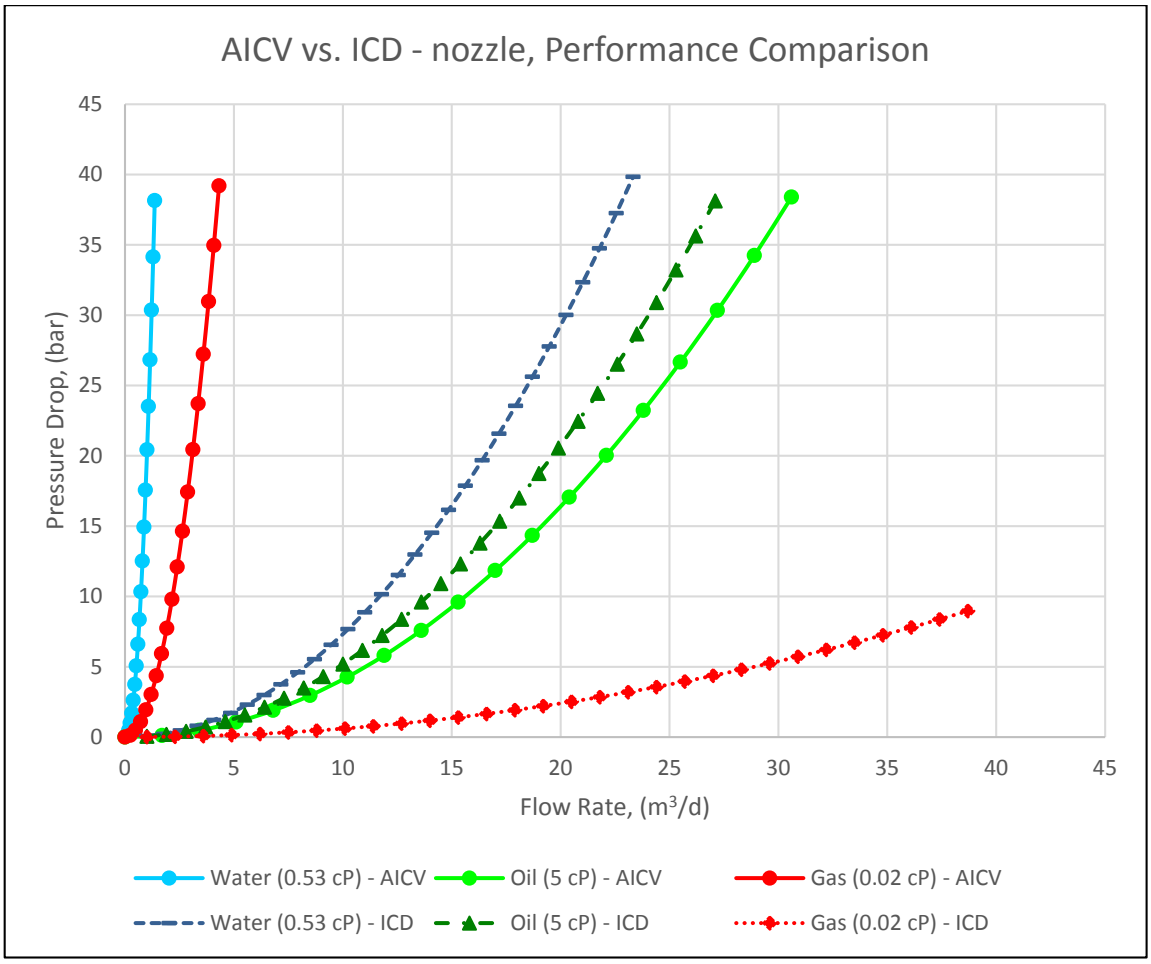

Figure 49: Comparison between AICV and ICD - nozzle performance characteristics

From Figure 49, it can be observed that the choking effect of water and gas is much higher for AICV compared to the ICD – nozzle, although they have the same flow rate exponent, (n=2). But the difference in proportionality constant (C) is high, therefore choking effect is higher for AICV compared to the ICD. Therefore, the AICV shows high sensitivity on the changing in the fluid properties (viscosity and density). On the other hand, the oil flow is very similar for both devices. Therefore, the choking effect, in order to stop the early breakthrough of unwanted fluids, is very similar.

5 Discussion

Following the results of performance testing of the AICDs described in the previous chapters, some of their differences are going to be compared and examined. In order to make the differences more clear, the performance is going to be separated by the control properties of the device. AFD is going to be compared with Wormhole AFD, and EquiFlow AICD, RCP valve and the AICV, are going to be compared also.

At the end of the Discussion chapter, table will be presented, which will gather all of the important parameters for all tested devices, including the performance data.

5.1 AICD Comparison

Starting from the AFD valve, as it is flow controller valve, it is going to be compared with the Wormhole AICD. Since the fluids performance relations, used in performance testing are mostly flow rate dependent, they are not much affected by the fluid properties. Based on that, and the device design, properties for keeping the flow rate in the certain boundaries are different. Wormhole AICD keeps the flow rate in predetermined limits (step change), by closing and opening pressure sensitive valves that are connected in series, with the labyrinth pressure drop flow pathway in between. On the other hand, AFD uses “hydraulic feedback principle”, with the pretension spring in its design for controlling the constant flow rate. Therefore, the AFD has a more smooth trend line in keeping the flow rate constant, compared to a more step change for the Wormhole AICD.

Since it has been shown that all of these three AICDs, EquiFlow AICD, RCP valve and the AICV, have improved performance compared to the ICD, they are going to be compared in between. Joined principle for all of them, is that viscosity is the main parameter on which the flow control is achieved. This comparison will include water, oil and gas flow for AICV and RCP, and just oil and water flow for the EquiFlow, since it is mainly water stopper valve, compared to the other two. Performance comparison for these AICDs is shown in Figure 50 below.

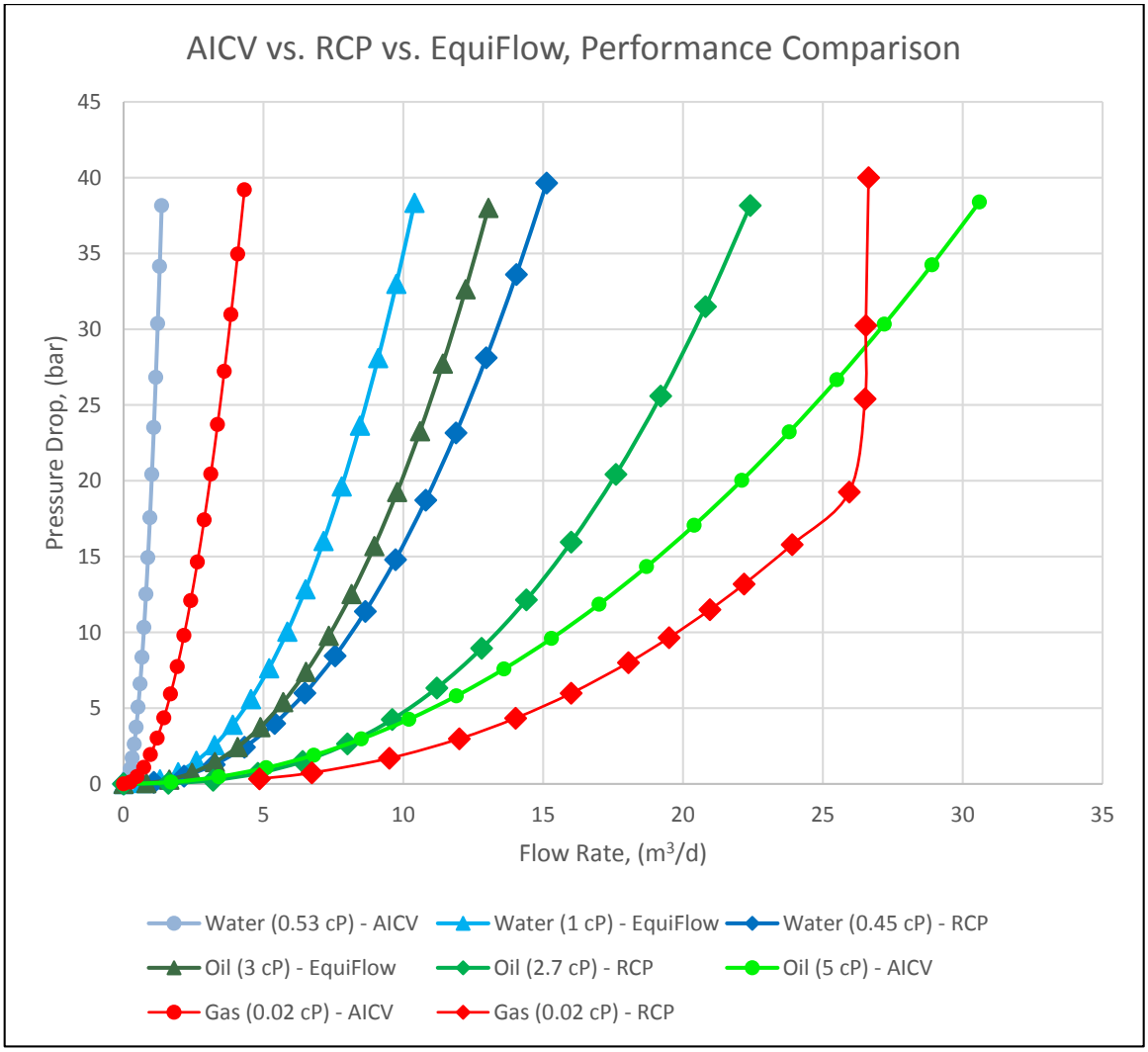

Figure 50: Performance Comparison between AICV, RCP and EquiFlow

From Figure 50, it can be seen that the water flow is choked the most with the AICV, than for EquiFlow and RCP valve at the end. As for the oil flow, it flows with less resistance through AICV, than through RCP valve and EquiFlow at the end. Looking at the gas flow through AICV and RCP valve, it is noticeable how the AICV chokes the production of gas almost immediately compared to the RCP valve, which needs some time. Nevertheless, both AICV and RCP almost completely stop the production of gas.

It can be concluded that, the EquiFlow AICD is mainly a water stopper device, and that both RCP and AICV, respectively, can be used both as a water and gas stopper devices. Also, what is important to mention, is that all of them are mainly viscosity dependent, and especially with the water inflow control, and that they are also flow controller devices in addition. Compared to the AFD and Wormhole AICD, which keep the flow rate relatively constant or in the limits, all of the other AICDs covered, have a flow control capability, in

order to prevent an early breakthrough. The difference between water and oil viscosity is crucial in order for these AICDs to work properly and in the proper range. All of them are made in different variants in order to cope with this problem.

The reason, because the performances are improving going from EquiFlow, up next to RCP and finally AICV, is the development period. AICV as the most recent device, is coping with the inflow issues more efficiently, incorporating more recent of the industry improvements and knowledge in its design.

5.2 Discussion of the Performance Data for AICDs

Performance date calculated for the most of the AICDs, is interesting to compare as one more indicator of their performances. By comparing the average values for proportionality constant (C) and flow rate exponent (n), it can also be seen that the AICV is the most efficient, then RCP, then EquiFlow and Equalizer Select (Table 7).

Table 7: Performance data (C, n), comparison for AICDs and ICD

	Average Proportinality Constant (C)	Average Flow Rate Exponent (n)
ICD	0.0432	2
AICV	4.4	2
RCP	0.03	2.6
EquiFlow	0.06	2.3
Equalizer Select	0.008	2.03

Analyzing this data the combination of the average (C) and average (n) as the flow parameters for the AICDs performance characteristics can be determined. Therefore, the effect of flow areas and velocity of the flowing fluid, based on the values of the average flow rate exponent (n), is highest for: RCP valve, EquiFlow, Equalizer Select and AICV, respectively. The choking effect of the AICDs, based on the average proportionality constant (C), and sensitivity to the change of the fluid properties (viscosity and density), going from the largest to the smallest are: AICV, EquiFlow, RCP valve and Equalizer Select.

AICV has the largest value of the average proportionality constant (C), and the same flow rate exponent (n) as the ICD – nozzle. Therefore, the AICV shows that it is the most sensitive to the change of the flowing fluid properties (viscosity primarily and density), providing the highest choking effect for certain fluids (water and gas). Although, it has a very similar flow area and velocity effect compared to the ICD – nozzle, due to the same value for (n).

RCP valve has lower proportionality constant (C) compared to the EquiFlow, therefore lower sensitivity to the change of the flowing fluid properties (viscosity and density), but the flow rate exponent (n) is considerably higher for RCP. High value for (n) for the RCP valve, shows that it is more sensitive to the changes of the flowing fluid velocity, and the effect of the flow area change. This proves the principles (Bernoulli's principle) covered for the RCP valve.

EquiFlow has higher value for the average proportionality constant (C) compared to the RCP valve, and the choking effect is slightly higher for the EquiFlow AICD, due to the change in fluid properties. The sensitivity to the effect of the flow area and velocity, compared to the RCP valve, is lower, due to the constant flow area of the EquiFlow. But still, the EquiFlow performance is mainly based on the change in the fluid viscosity.

Equalizer Select has shown as the least efficient, but the strength of it is in its adjustability, and simplicity. The flow rate exponent (n), is almost the same as for the ICD – nozzle, which shows that the flow area and flowing velocity effects are similar to the ICD - nozzle. On the other hand, proportionality constant (C) for the Equalizer Select is different for different FRR settings. For higher FRR 6.4, the proportionality constant (C) is the highest for the device, and therefore the most sensitive on the fluid properties. For lower FRR settings, the proportionality constant (C) is lower, due to the lower resistance to flow.

5.3 AICDs Sensitivity to the Different Reservoir Properties

Every AICD is good in its own way. Depending on the reservoir type, different AICDs can be applied. It is difficult to distinguish which is the good or bad. Some of them are primarily water stoppers, others primarily gas stopper or flow rate controller devices. But, in some cases, it is good to allow a bit higher amount of produced water, to carry the residual oil with it. So choking the water production is not necessarily good every time. As for the gas stopping effects, it is different, it is usually good to install gas stopping autonomous valve in the combination with the oil reservoir with a gas cap. For the flow controller devices, it is more straightforward, they can be beneficial where the keeping the flow rate in some limits is necessary. In order to get the most from the oil recovery perspective, everything has to be considered, starting from reservoir properties as the most important. Afterwards, the best option from the inflow control perspective, can be analyzed, considered, and installed in the completion phase.

Another thing to mention, is the effect of the emulsions on the performance of the AICDs. For example, emulsion of water and oil, can increase the viscosity of the flowing fluid, and therefore the effect of the AICD needs to be reconsidered, especially if they are mostly viscosity dependent.

Since this topic goes out of the scope of this thesis, therefore it requires a separate analysis.

5.4 Overview of Analyzed AICDs

In the table 8 below, a final overview of the working principles, physics properties of the AICDs and ICD, together with the flow rate property is presented.

Table 8: Final overview of the AICDs together with ICD

	Working Principle	Physics Property Dependance	Flow Rate Property
ICD	Nozzle	Density	Q^2
AFD	Movable Disc, Spring, Pressure	Flow Rate, Density	Const. Q
Wormhole AICD	Labyrinth pathways, Shut – off valves	Flow Rate, Viscosity	Q in predetermined limits
Floating – Flapper Valve	Floating – Flapper, Nozzle	Buoyancy, Density	Q^2
Equalizer Select	Selectable Labyrinth Pathways, Nozzles	Density, Viscosity	$Q^{2.03}$
EquiFlow AICD	Fluidic Diode (Vortex), Nozzle	Viscosity, Density	$Q^{2.3}$
RCP Valve	Floating Disc	Viscosity, Density	$Q^{2.6}$
AICV	Floating Disc, Laminar, Turbulent Flow Restrictors	Viscosity, Density	Q^2

6 Conclusion

Considering flow performance properties of all of the covered AICDs and the flow performance properties of a regular ICD – nozzle, it can be concluded that AICDs have improved performance compared to the ICD – nozzle. This has been concluded with the testing each one of them, with the flow of the same fluids, and comparing them.

During developing of these performances and comparing them, the following conclusions are made:

- AICD showed improved efficiency compared to the ICD – nozzle;
- Not every AICD is able to choke both water and gas;
- AICDs are designed with a wide range of specifications, in order to cover a wider range of fluids with different properties;
- AFD and Wormhole AICD are designed from a flow control perspective, to keep the constant flow rate, compared to the others;
- Equalizer Select has different choking options through FRR settings, and it is dependent on detailed reservoir property analysis, especially permeability distribution;
- EquiFlow AICD is designed mainly to be water stopper valve, and it is mainly sensitive to the fluid viscosity, so its efficiency in light oil reservoirs is questionable;
- RCP valve is designed to mainly be a gas stopper valve, it is controlled with the fluid viscosity, although it is possible to use it in heavy oil reservoirs as a water stopper valve, due to the wider viscosity ranges between water and oil;
- AICV, is the next step in development from RCP valve, since it is the viscosity and density controlled, it can handle both water or gas inflow, due to its unique design which incorporates both laminar and turbulent flow restrictors. It can be adapted to the wide range of fluid properties;
- Equalizer Select, EquiFlow, RCP and AICV also have a flow control function in addition to its main function, in order to prevent an early breakthrough of unwanted fluids.

7 References

Aadnoy, B. S. (2010). *Modern well design*: University of Stavanger, Stavanger, Norway: CRC Press.

Aakre, H., Halvorsen, B., Werswick, B., & Mathiesen, V. (2013). *Smart well with autonomous inflow control valve technology.* Paper presented at the SPE Middle East Oil and Gas Show and Conference.

Aakre, H., Halvorsen, B., Werswick, B., & Mathiesen, V. (2014). *Autonomous Inflow Control Valve for Heavy and Extra-Heavy Oil.* Paper presented at the SPE Heavy and Extra Heavy Oil Conference: Latin America.

Abdelfattah, T. A., Banerjee, S., Garcia, G. A., & Nguyen, H. T. (2012). *Effective use of passive inflow control devices to improve the field development plan.* Paper presented at the SPE Deepwater Drilling and Completions Conference.

Akbari, M. (2014). *Analyzing the Correlations in Generalization of the Reservoir Information in a Well Completion Design Optimization using ICD's along the Horizontal section of a Wellbore.* Paper presented at the SPE 170279 presented at the SPE Deepwater Drilling and Completions Conference, Galveston, texas, USA.

Akbari, M., Gonzalez, J. R., & Macklin, N. (2014). *Considerations for Optimum Inflow Control Devices (ICDs) Selection and Placement in Horizontal Sections (Russian).* Paper presented at the SPE Russian Oil and Gas Exploration & Production Technical Conference and Exhibition.

Banerjee, S., Abdelfattah, T. A., & Nguyen, H. T. (2013). *Benefits of Passive Inflow Control Devices in a SAGD Completion.* Paper presented at the SPE Heavy Oil Conference-Canada.

Bowen, E. G., & Aadnoy, B. S. (2014). *A Quasi Intelligent Flow Control Device for Water Injectors.* Paper presented at the IADC/SPE Asia Pacific Drilling Technology Conference.

Crow, S. L., Coronado, M. P., & Mody, R. K. (2006). *Means for passive inflow control upon gas breakthrough.* Paper presented at the SPE Annual Technical Conference and Exhibition.

Delia, S., Chertenkov, M., Zhakovschikov, A., Matsashik, V., Zhuravlev, O., & Shchelushkin, R. (2015). *Field Tests of a New Generation of Flow Control Unit Able to Prevent the Gas Breakthrough in Oil Wells (Russian).* Paper presented at the SPE Russian Petroleum Technology Conference.

Ellis, T., Erkal, A., Goh, G., Jokela, T., Kvernstuen, S., Leung, E., . . . Vorkinn, P. B. (2009). Inflow Control Devices—Raising Profiles. *Oilfield Review, 21*, 30-37.

Eltaher, E. K., Muradov, K., Davies, D. R., & Grebenkin, I. M. (2014). *Autonomous Inflow Control Valves-their Modelling and" Added Value".* Paper presented at the SPE Annual Technical Conference and Exhibition.

Fripp, M., Zhao, L., & Least, B. (2013). *The Theory of a Fluidic Diode Autonomous Inflow Control Device.* Paper presented at the SPE Middle East Intelligent Energy Conference and Exhibition.

Garcia, G. A., Nguyen, H. T., & Serrano, J. (2010). *Passive Inflow Control Device Flow Performance Characterization*: Baker Oil Tools.

Garcia, L., Coronado, M. P., Russell, R. D., Garcia, G. A., & Peterson, E. R. (2009). *The first passive inflow control device that maximizes productivity during every phase of a well's life.* Paper presented at the International Petroleum Technology Conference.

Greci, S., Least, B., Aitken, L. A., & Ufford, A. (2014). *Plugging Testing Confirms the Reliability of the Fluidic Diode-Type Autonomous Inflow Control Device.* Paper presented at the SPE Deepwater Drilling and Completions Conference.

Halvorsen, M., Elseth, G., & Nævdal, O. M. (2012). *Increased oil production at Troll by autonomous inflow control with RCP valves.* Paper presented at the SPE Annual Technical Conference and Exhibition.

Halvorsen, M., Madsen, M., Vikøren Mo, M., Isma Mohd, I., & Green, A. (2016). *Enhanced Oil Recovery On Troll Field By Implementing Autonomous Inflow Control Device.* Paper presented at the SPE Bergen One Day Seminar.

Iqbal, F., Iskandar, R., Radwan, E., Abbas, H., Douik, H., Least, B., & Mohamed, Z. (2015). *Autonomous Inflow Control Device-A Case Study of First Successful Field Trial in GCC for Water Conformance.* Paper presented at the Abu Dhabi International Petroleum Exhibition and Conference.

Isma Mohd, I. (2014). *Autonomous Inflow Control Devices. Modelling and Porting into Reservoir simulators.* Passive Inflow Control Technology Forum Abu Dhabi, UAE.

Lauritzen, J. E., & Martiniussen, I. B. (2011). *Single and Multi-phase Flow Loop Testing Results for Industry Standard Inflow Control Devices.* Paper presented at the Offshore Europe.

Least, B., Greci, S., Konopczynski, M., & Thornton, K. (2013). *Inflow Control Devices Improve Production in Heavy Oil Wells.* Paper presented at the SPE Middle East Intelligent Energy Conference and Exhibition.

Least, B., Greci, S., Wilemon, A., & Ufford, A. (2013). *Autonomous ICD Range 3B Single-Phase Testing.* Paper presented at the SPE Annual Technical Conference and Exhibition.

Mathiesen, V., Werswick, B., & Aakre, H. (2014). *The Next Generation Inflow Control, the Next Step to Increase Oil Recovery on the Norwegian Continental Shelf.* Paper presented at the SPE Bergen One Day Seminar.

Mathiesen, V., Werswick, B., Aakre, H., & Elseth, G. (2011). *Autonomous Valve, A Game Changer Of Inflow Control In Horizontal Wells.* Paper presented at the Offshore Europe.

Mayer, C. S. J., Spiecker, M., Shuchart, C. E., Burkey, R. C., Ufford, A., & Brysch, J. (2014). *Multiphase Flow Performance of Inflow Control Devices-Characterizing Downhole Flow Behavior in Lab Experiments.* Paper presented at the Abu Dhabi International Petroleum Exhibition and Conference.

Volkov, V. Y., Alexander P. Skibkin, P., Oleg N. Zhuravlev, P., & Roman V. Schelushkin, P. (2014). Adaptive Inflow Control System. *Bauman Moscow Technical State University; Wormholes Ltd.*

Voll, B. A., Ismail, I. M., & Oguche, I. (2014). *Sustaining Production by Limiting Water Cut and Gas Break Through With Autonomous Inflow Control Technology.* Paper presented at the SPE Russian Oil and Gas Exploration & Production Technical Conference and Exhibition.